イジングモデルの自己相似性および臨海緩和について(修士論文(1987年度))

AUTHOR(S):

伊藤, 伸泰

CITATION:

伊藤, 伸泰. イジングモデルの自己相似性および臨海緩和について(修士論文(1987年度)). 物性研究 1988, 50(4): 723-768

ISSUE DATE:

1988-07-20

URL:

http://hdl.handle.net/2433/93122

物性研究50－4（1988－7）

修士論文（1987年度）

イジングモデルの自己相似性および臨界緩和について

東京大学　理学部　物理　伊藤伸泰

序文

この論文は3つの章からなる。いずれの章もスピン系の臨界現象について扱う。

第1章では、イジングモデルの配位の自己相似性について調べる。第2章では、2次元イジングモデルの臨界緩和を調べ、動的臨界指数を数値的に求めた結果を示す。第3章では、CAM理論をハイゼンベルグモデルに応用した結果を示す。

初めの2つの章では、モデルの解析手段として、電子計算機によるモンテカルロ法を使っている。第1章では、汎用機とベクトル計算機（スーパーコンピュータ）を使用した。第2章では、泰地真弘人（東大理物理）氏とともに開発した、イジングモデルのモンテカルロ専用計算機を使用した。技術的な詳細を、各章のappendixに記した。

1946年に最初の電子計算機ENIACが完成して以来、計算機は急速な発達を続けている。そして、あらゆる分野に大きな影響を与え続けている。今日の物理学も計算機の持つ強力な計算能力と情報処理能力の影響を受けている。

物理学は、世の中のあらゆる現象の理解を目的としている。ここで、理解するという事は人間の能力に相対的なものである。一方、計算機の出現によって、人間の能力のある部分（数値計算や記録保持など）を質、量ともに拡大しつつある。このため、計算機の出現によって従来とは異質の「理解」が成立しうるであろう。そして、人間の自然に対する理解がいっそう深まる事を期待している。

各章の前に付した日本語の要旨は、読者の便宜と物性研究編集部の方針とを考慮して付したものである。

Contents

第１章　要旨

二次転移点で系の自由エネルギーは、スケール変換のもとで自己相似に振舞う。自由エネルギーは、統計平均をとって得られる量である。自由エネルギーなどの統計平均した量の自己相似性は、次の意味での系の各配位の自己相似性に由来する事が分った。それは、臨界点での出現頻度の大きい配位は、磁化で見て一定のフラクタル次元Ｄを持っている、という事である。

臨界点での典型的な配位に対してスケール変換を施した際の磁化の変化が、スケールに対してべき関数で振舞うのである。スケール変換はブロックスピン変換である。つまり、全系を一辺ｂの（超）立方体に切り分け、各（超）立方体中の磁化が正ならば＋１のスピンに、負ならば－１のスピンに置き換える。また、０ならば、確率１／２で＋１または－１とする操作である。

系が２、３、４次元の場合には、ｄを系の次元、β、γ、νを自発磁化、帯磁率、相関長の臨界指数として、

$$D = d - \beta / \nu = (d + \gamma / \nu) / 2$$

が成立する。これはハイパースケーリング則

$$\nu d = 2 \beta + \gamma$$

を含意する。

一方、ハイパースケーリング則の成立しない５次元以上の場合は、系をスケールする長さの臨界指数は相関長の臨界指数νではなく、

$$\nu ' = 2 / d$$

であることが推定される。

臨界点からずれた場合の配位の次元は、低温側では秩序相のため格子の次元ｄが得られ、高温側ではランダム相のため中心極限定理より予想されるｄ／２が得られる。

appendixにモンテカルロシミュレーションをベクトルコンピュータで効率よく実行させる方法について記す。

2 *Chapter 1. Fractal Configurations*

1-1. Critical Phenomena and Fractal Nature

Many studies have been made for the critical phenomena using the droplet or cluster pictures and from a view-point of percolation problems.[1-1)~1-14)] They are based not on configurations as a whole but on clusters in the configurations. This cluster picture works good near the critical point. However if we treat the system very close to the critical point, the definition of the cluster of this picture becomes vague and difficult. The success of the renormalization group method[1-15)~1-18)] suggests that the self-similarity can be studied more directly by looking at the configurations. The concept of fractals for self-similar systems was proposed by Mandelbrot.[1-19)] He and others studied critical phenomena on fractal lattices and revealed some important relations between fractal dimensions of a lattice and critical phenomena on it.[1-20,1-21)]

Suzuki[1-22)] has discussed the relation between critical phenomena and the fractal nature of each configuration at the critical point. His argument is briefly reviewed in the following.

If the largest cluster of the relevant configuration has the volume L^D (where L denotes the size of the system) at the critical point, the following two relations can be derived with the use of the finite size scaling [1-23)~1-25)]:

$$\beta = -\nu(D-d) \qquad and \qquad \gamma = \nu(2D-d).$$

(where d, β , γ and ν denote the dimensionality of the system, and critical exponents of magnetization, susceptibility and correlation length, respectively). These relations yield automatically the hyperscaling relation $d\nu = 2\beta + \gamma$. In this argument, he expected that the magnetization at the ordered phase ($T < T_c$) was connected with the percolated clusters at the transition point ($T = T_c$).

Now a new theory stimulated by the above mentioned intuitive argument is discovered here. In this theory, the fractal dimensionality D is defined using the magnetization of the system and the same argument as Suzuki's original argument leads us to the hyperscaling with the help of finite size scaling. The detail of our theory will be explained in the succeeding sections.

The hyperscaling relation is essential to understand the non-classical behavior of the system. Therefore to clarify many aspects of the hyperscaling relation is fundamental in the study of critical phenomena and field theory. Our new theory reveals some important aspect of the hyperscaling and finite size scaling exponent.

We have confirmed the fractalness of the two-, three- and four-dimensional Ising models at the critical point without directly referring to the distribution of clusters. Our method is, in a sense, an extension of the cluster approaches.[1-1)~1-14)] It has some theoretical and practical advantages (which will be shown in the succeeding sections) compared with the cluster approaches, because it is directly connected with the microscopic Hamiltonian through the magnetization of the configuration and fractal picture works at the critical point, although the cluster pictures run into difficulties. Practically it is easy to test this by Monte Carlo simulations. It has an analogy to the real space renormalization group transformation and the Monte Carlo renormalization group method.

1-2. Fractal Nature of Each Configuration

In the present paper we verify the following conjecture: in the Ising models at the critical point, the magnetization of each configuration which has appreciable Boltzmann probability shows a power law behavior with respect to L, the linear size of the system, i.e., $M(L) \sim L^D$ under the majority rule scale transformation. This conjecture insists the fractalness of each configuration. Each configuration of the system with linear size L is mapped to another configuration of the corresponding size L/b system by the scale transformation with scale factor b. At the critical point the emergence probability, or Boltzmann probability is also correctly mapped, because the critical point of the Ising model is a fixed point of this scale transformation in the renormalization group scheme. Therefore, the magnetization of the original system is proportional to L^D and that of the scaled system to $(L/b)^D$. This expresses the very fractalness of each configuration.

This conjecture yields the hyperscaling if we uses the finite size scaling argument. Assuming this conjecture and the finite size scaling, the total magnetization M_{tot} of the configuration of the relevant system with linear size L, which is important to statistical average, is proportional to L^D. When the finite size scaling argument[22),23)] is applied, the statistical average $< m >$ of the magnetization per site, m, has $t^{-\nu(D-d)}$ dependence on t, where $t = T - T_c$. Therefore

$$\beta = -\nu(D-d) \qquad or \qquad D = d - \beta/\nu. \tag{1-1}$$

On the other hand, the susceptibility per site, χ , is

$$\chi \sim < m^2 > \sim L^{2D-d} \sim t^{-\nu(2D-d)}$$

at temperatures higher than the critical point. Therefore we obtain

$$\gamma = \nu(2D-d) \qquad or \qquad D = (d+\gamma/\nu)/2. \tag{1-2}$$

If we eliminate the parameter D from (1-1) and (1-2), then we obtain the hyperscaling relation $d\nu = 2\beta + \gamma$. If this fractal picture is correct, the exponent ν of the correlation length and the exponent ν' appearing in the finite size scaling must be different in the higher dimensions than four. With this notation of ν' the scaling relation $d\nu' = 2\beta + \gamma$ is obtained from fractal picture. Therefore ν' is equal to $2/d$ for mean field behavior in four or more dimensions. For example in five dimension the values of ν' is estimated from this relation is 2/5 which is consistent with the Monte Carlo results by Binder[1−26)]. The possibility of ν'=2/d is already pointed out by many authors[1−27)] and our argument supplies intuitive picture for their argument. We have examined the above-mentioned conjecture using the Monte Carlo sampling method. Obtained configurations are used to measure the fractal dimensionality D at and near the critical point. The details of the simulation are given in the next section. If the relevant system is really scale-invariant, the dimensionality D is constant irrespective of the scale factor used in the scale transformation.

Our scale transformation is constructed by the ordinary majority rule or the block counting method. This transformation removes, from the configuration, the

clusters which are smaller than the scale used by the transformation. Thus our theory may include the ordinary cluster theories of critical phenomena which are too phenomenological to be explained by the principles of statistical mechanics. Our theory is easier to be treated with first principles, because it is formulated using the total magnetization of the system and the total magnetization is theoretically and numerically easier to treat than the clusters in the system.

1-3. Test of the Conjecture by Monte Carlo Method

Our procedure is summarized as follows. Firstly configurations are generated by Monte Carlo simulations. If one continues an enough number of Monte Carlo steps, the obtained distribution of configurations follows the equilibrium distribution. Secondly using the scale transformation, the fractal dimensionality of the relevant system is measured with many scales.

The definition of the fractal dimensionality D is given by

$$D(b) = \frac{\log \frac{M_{tot}(1)}{M_{tot}(b)}}{\log b}, \qquad (1-3)$$

where $M_{tot}(x)$ is the total magnetization of the configuration which is obtained by the scale transformation with scale x from the original configuration. If the linear size of the original configuration is L, $M_{tot}(b)$ is the total magnetization of one of the configurations of the system whose linear size is L/b, while $M_{tot}(1)$ is the total magnetization of the original configuration. One may suspect that the D defined by (1-3) may be accompanied with the effect of the transient effect, because fractal objects often have their own scale regions in which the system display scale-invariant character.[1-28] In our cases, however, this effect turned out to be rather small. The existence of the infrared cut off (the system size) can produce some effects on the fractal behavior. Therefore the definition (1-3) is appropriate for our purpose.

If each spin in the system takes the $+1$ or -1 state randomly, the D defined by (1-3) is $d/2$ as shown in (1-A-1), where d is the dimensionality of the relevant lattice. In this case, the short-range correlation can make some transient behavior of $D(b)$. This is irrelevant to the present work, because we are not so much interested in the case in which the temperature is not the critical point.

At temperatures higher than the critical point, such a random situation is expected to occur. If the scale factor b is large enough, $D(b)$ will approaches $d/2$.

At temperatures lower than the critical point, $D(b)$ will approach d if b is large enough, because the system is in the ordered state.

Just at the critical point, $D(b)$ is expected to be equal to $D = d - \beta/\nu$ irrespective of b.

To avoid the transient fractal effect and to obtain the exact values of D, we had better to try the scale transformation repeatedly for the scale transformed configuration. The estimation of D is given by

$$D_n(b) = \frac{\log \frac{M_{n-1}(b)}{M_n(b)}}{\log b}, \qquad (1-4)$$

where M_n is the total magnetization of the configuration after n-times scale transformation with scale factor b.

We have examined the fractalness of the two-, three- and four-dimensional Ising models on square and simple cubic lattices with cyclic boundary conditions in all directions. Our Monte Carlo algorithm was the Metropolis method.[1-29] Two kind of fractal dimensionalities are estimated using (1-3) and (1-4) for two- and three-dimensional systems. For four-dimensional case only the that of (1-3) is tried. Figure 1-1 is one of the configurations of the 1024^2 Ising system at the critical point. This figure displays self-similarity or fractalness. This fractalness is the fractal property of the magnetization. It should be remarked that only the up (or down) sites of the relevant configuration (for example, black or white sites in Fig. 1-1) do not show fractal dimensionality $D = d - \beta/\nu$ but we get d instead of D by the majority rule scale transformation, which was explicitly confirmed numerically in the two-dimensional case.

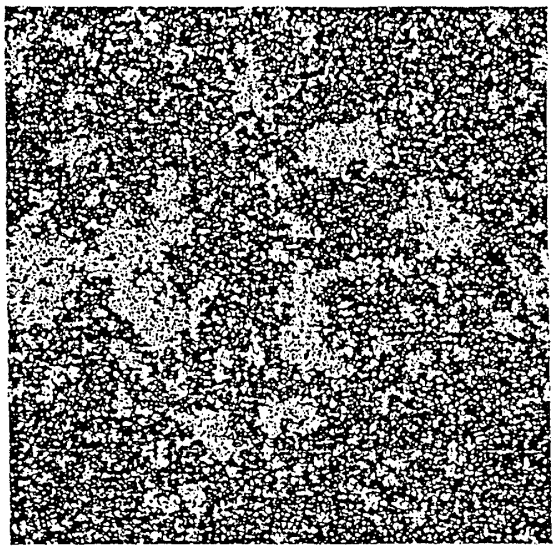

Fig. 1-1.
A typical configuration of the 1024^2 Ising system at the $K = K_c = 0.4407$ is shown. Up-spin sites are displayed by black dots. One can observe a self-similar structure.

1-3-1 Two-Dimensional Case

In this case, we have studied not only at the critical point, but also at other temperatures around the critical point. The system studied here was the 64^2 square lattice Ising model with cyclic boundary conditions in all directions. The expected values of the $D(b)$ defined by (1-3) are the following:

$$\begin{aligned} \lim_{b\to\infty} D(b) &= 1 \qquad for \quad K < K_c \quad (T > T_c), \\ D(b) &= 1.875 \quad for \quad K = K_c \quad (T = T_c), \\ \lim_{b\to\infty} D(b) &= 2 \qquad for \quad K > K_c \quad (T < T_c), \end{aligned} \tag{1-5}$$

where K is J/k_BT, k_B is the Boltzmann constant, T is the temperature and J is defined in the following Hamiltonian of the system:

$$\mathbf{H} = -J \sum_{|i-j|=1} S_i S_j \qquad (S_i = \pm 1).$$

The result is shown in Fig. 1-2. From this figure, the behavior described in (1-5) is clearly observed.

The feature of the system at the critical point is given in the following. Figure 1-3 shows the behavior of the magnetization at the critical point with increase of Monte Carlo steps. Most of the configurations take such values of the magnetization as are near the maximum in magnitude. The distribution of this magnetization is given in the Fig. 1-4. The magnetization distribution of finite systems was also studied by Binder.[1-30] Figure 1-5 shows the correlation function of the system of 64^2 at the critical point. The correlations for small distances are consistent with exact calculations by Ghosh and Shrock[1-31] From this figure, we can observe that the system recovers the Euclidean rotational symmetry (i.e., $O(2)$) at the critical point from the small distances. The rotational symmetry for the large distances in thermodynamic limit can be appreciated from the exact forms of correlation functions for lattice directions and asymptotic form for diagonal direction[1-32]. The first five points along the lattice axis yield $\eta \simeq 0.23$ (and Onsager- Yang's exact value of η is $1/4$), where η is defined by the correlation function $\Gamma(r) \sim r^{-(d-2+\eta)}$ at the critical point. Figure 1-6 also shows the correlation function at the critical point for the system of 1024^2. From these results we have obtained very good value $\eta \simeq 0.25$, by Monte Carlo simulations at the critical point, because one can use a great number of spin pairs in each configuration.

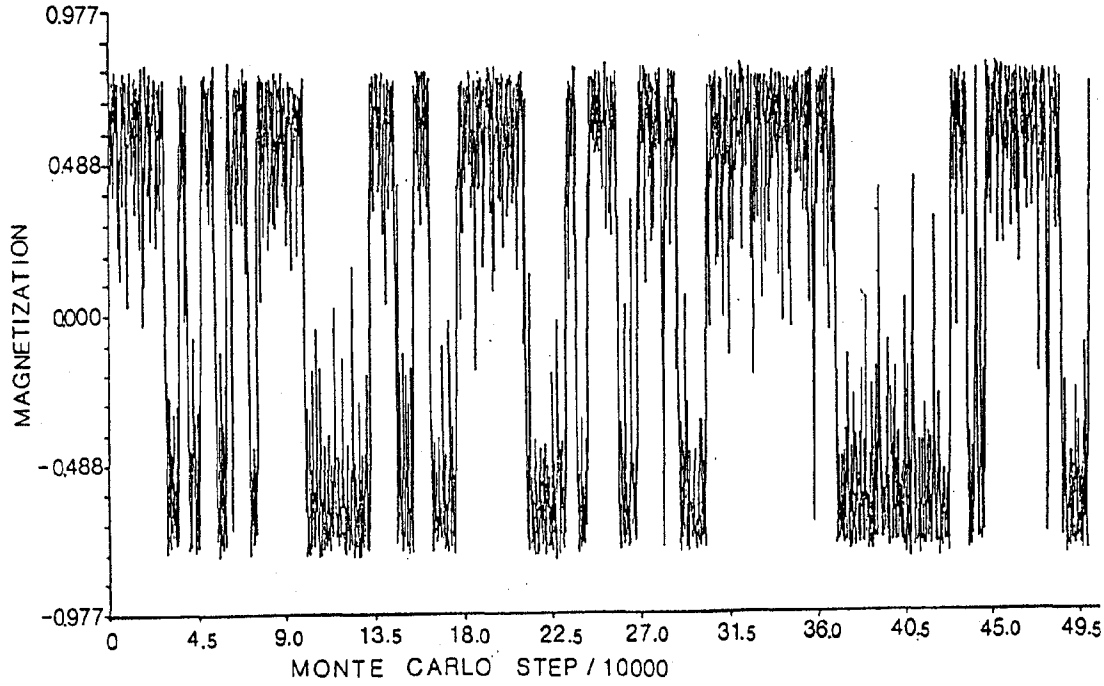

Fig. 1-3 The time evolution of the magnetization per spin is shown for the 64^2 system at the critical point. Configurations with either positive or negative magnetizations are dominant, and those with zero magnetization are scarce.

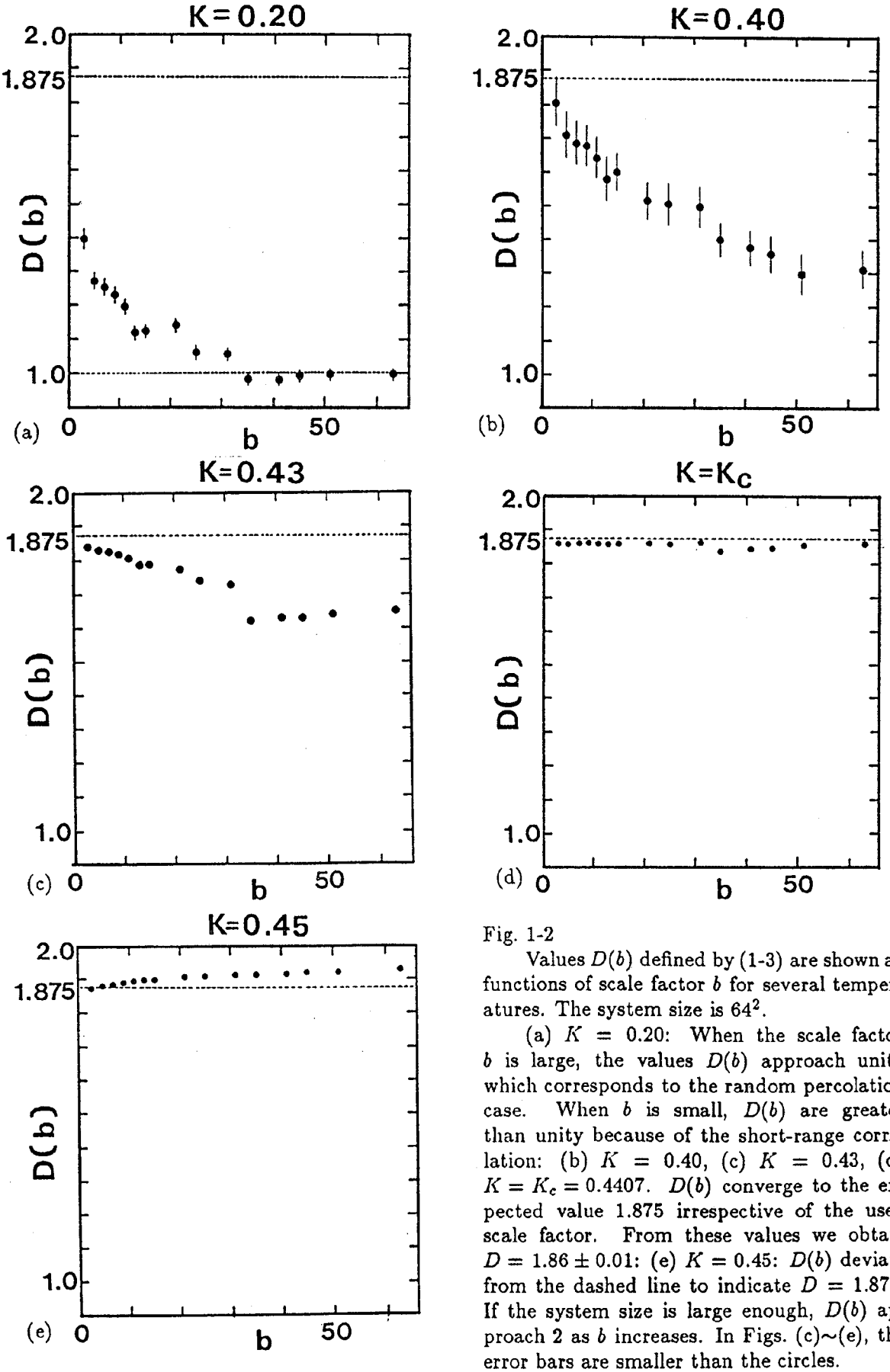

Fig. 1-2

Values $D(b)$ defined by (1-3) are shown as functions of scale factor b for several temperatures. The system size is 64^2.

(a) $K = 0.20$: When the scale factor b is large, the values $D(b)$ approach unity which corresponds to the random percolation case. When b is small, $D(b)$ are greater than unity because of the short-range correlation: (b) $K = 0.40$, (c) $K = 0.43$, (d) $K = K_c = 0.4407$. $D(b)$ converge to the expected value 1.875 irrespective of the used scale factor. From these values we obtain $D = 1.86 \pm 0.01$: (e) $K = 0.45$: $D(b)$ deviate from the dashed line to indicate $D = 1.875$. If the system size is large enough, $D(b)$ approach 2 as b increases. In Figs. (c)~(e), the error bars are smaller than the circles.

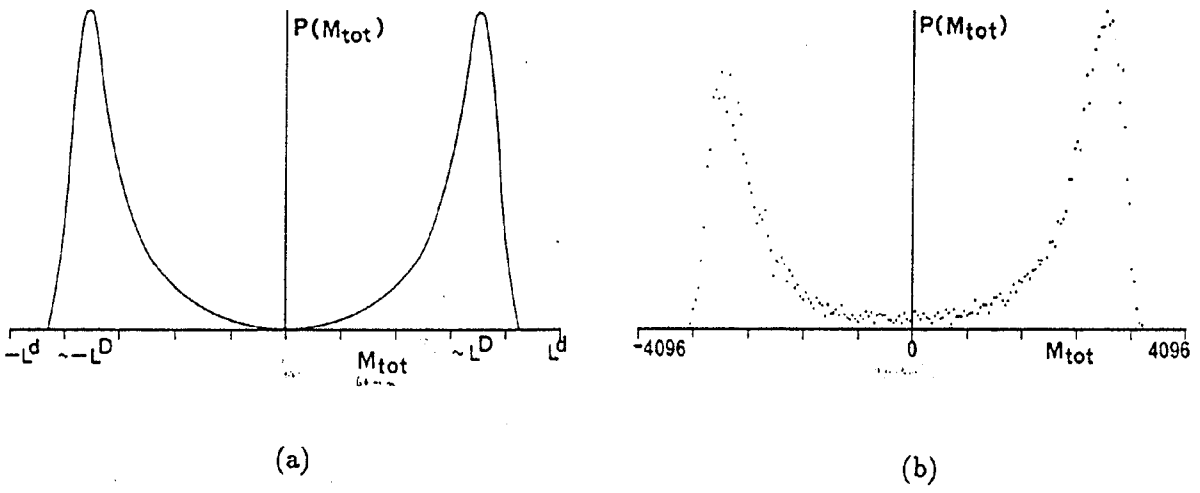

Fig. 1-4 The probability distribution function, $P(M_{tot})$, of the total magnetization, M_{tot}, of the system at the critical point is shown: (a) is a schematic figure of $P(M_{tot})$ for the system size L. and (b) denotes $P(M_{tot})$ corresponding to Fig. 1-3. The small asymmetry of (b) is due to the scarce Monte Carlo steps.

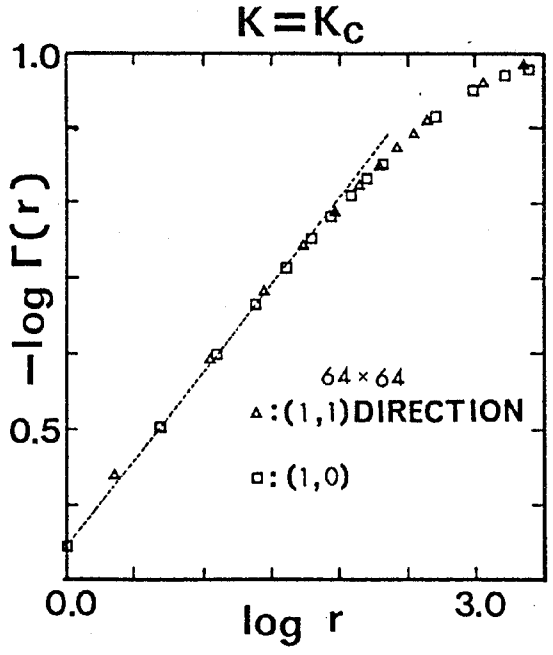

Fig. 1-5
Log-log plot of the correlation function at K_c obtained by Monte Carlo simulations for the 64^2 system is shown. The dotted line represents
$-\log < S_0 S_R >= 0.234 \log R + 0.341$.
This yields $\eta \simeq 0.23$.

Figure 1-7 shows the behaviors of $D(b)$ for some values of b at the early stage of the simulation. The initial condition is that all sites are up. The $D(b)$ converges to the expected value $D = 1.875$ very rapidly. Of course, for larger scale factors,

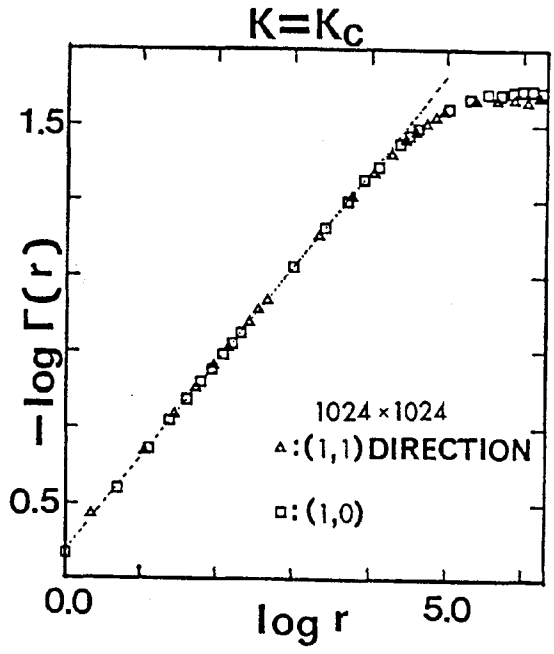

Fig. 1-6
A plot similar to Fig. 1-5 for the the system of 1024^2 is shown. The dotted line corresponds to
$-\log < S_0 S_R >= 0.253 \log R + 0.367$.
This yields $\eta \simeq 0.25$.

a larger number of steps are needed to reach equilibrium. These phenomena were also observed by Kikuchi and Okabe [1−33] during their Monte Carlo renormalization calculations. The reason why D reaches its equilibrium value so rapidly is understood by noting that there are so many blocks that their average has little fluctuation.

The other definition of dimensionality, (1-4), is also tried. The scale transformation is tried repeatedly to the original configuration to get rid of the transient effect. The scale factor used here is two. If the number of up sites and down sites in a box is equal, the block spin is selected using random numbers. We adopt up spin and down spin with equal probability in such a case. Figure 1-8 shows the behavior of $D_n(2)$ for n = 1,2,3,4,5 and 6. From this figure, the same behavior with Fig. 1-2 is observed. The values of $D_n(2)$ at the critical point are better than the $D(b)$ compared with the expected value 1.875

1.3.2 Three-Dimensional Case

In the three-dimensional case, we have also studied two definitions of fractal dimensionalities. The critical point of the Ising model on the cubic lattice is estimated by the Monte Carlo renormalization[1−32], finite-size scaling analysis[1−35] and high temperature expansion calculation[1−36] to be about $K_c = 0.2217$. The expected fractal dimensionality is estimated by the results of two different theories. The fractal dimensionality D is estimated to be 2.480 ± 0.007 from the high-temperature expansion[1−37] and 2.485 ± 0.004 from field theoretic calculations[1−38].

Firstly, the results of the values of D by (1-3) are given in Fig. 1-9. The system size is 64^3. The expected behavior is obtained. namely, the D approaches $d/2 = 1.5$ in the paramagnetic phase and to $d = 3$ in the ferromagnetic phase. Just at the critical point, the values of D are about 2.48 which is the expected value.

The dynamical behavior of D is also studied. The values of D in the first 50

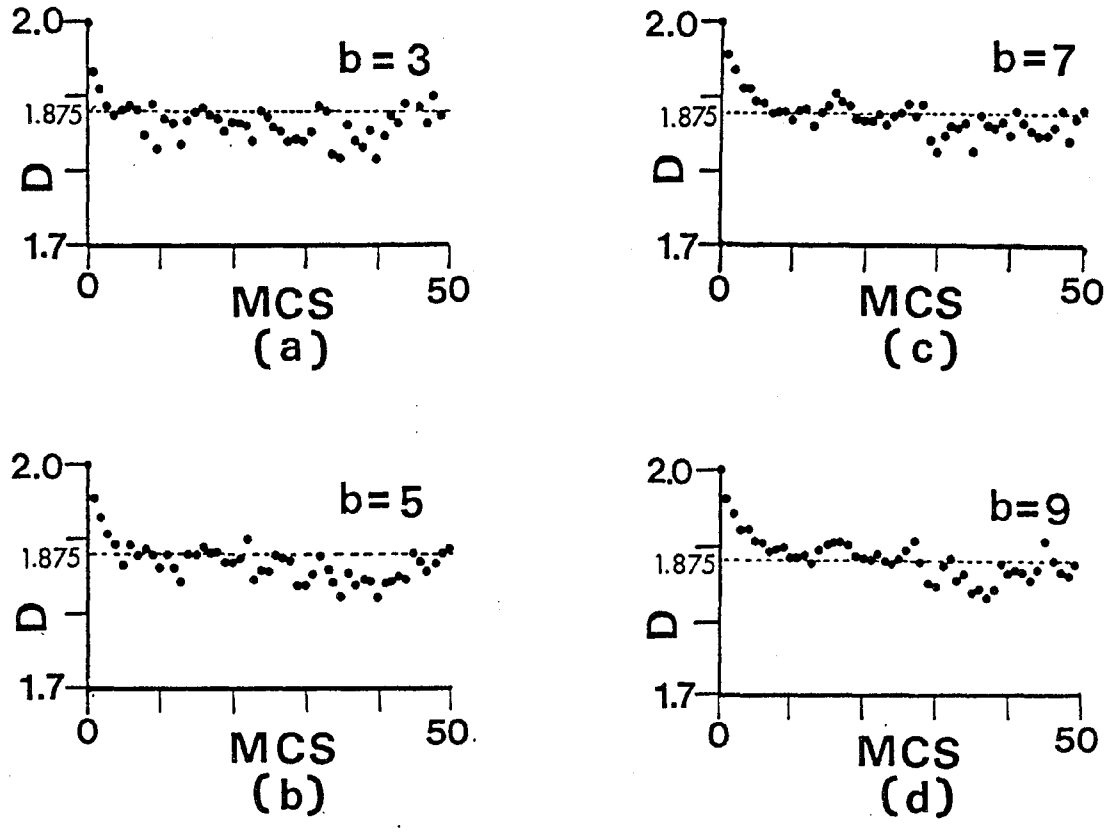

Fig. 1-7 The behaviors of $D(b)$ at the beginning of the simulations are shown: $K = K_c = 0.4407$ and the system size is 64^2. (a) $b = 3$, (b) $b = 5$, (c) $b = 7$, (d) $b = 9$. The relaxation of $D(b)$ is very fast. Of course, the relaxation time becomes longer, as the scale factor becomes larger.

Monte Carlo steps with the all-up initial state are shown in Fig. 1-10. The used scale is $b = 3$ and the system size is also 64^3. The result is given in Fig. 8.

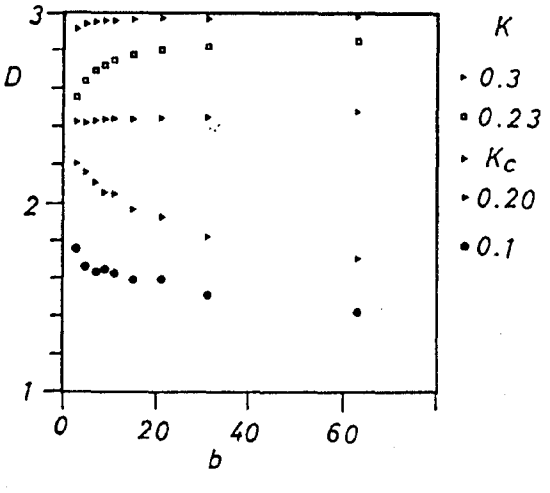

Fig. 1-9
The results of $D(b)$ for three dimensional 64^3 system.

Secondly the values of $D_n(2)$ by (1-4) are shown in Fig. 1-11. The behavior of

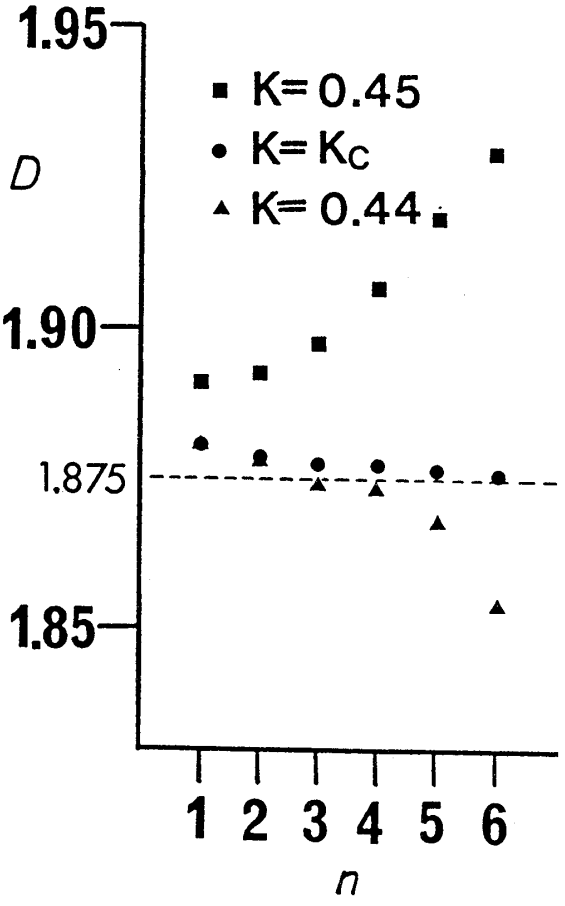

Fig. 1-8
The behavior of $D_n(2)$ in two dimensional 128^2 lattice for three temperatures around the critical point are shown. The feature is almost the same as Fig. 1-2. The values for critical temperature are, however, closer to the expected value 1.875.

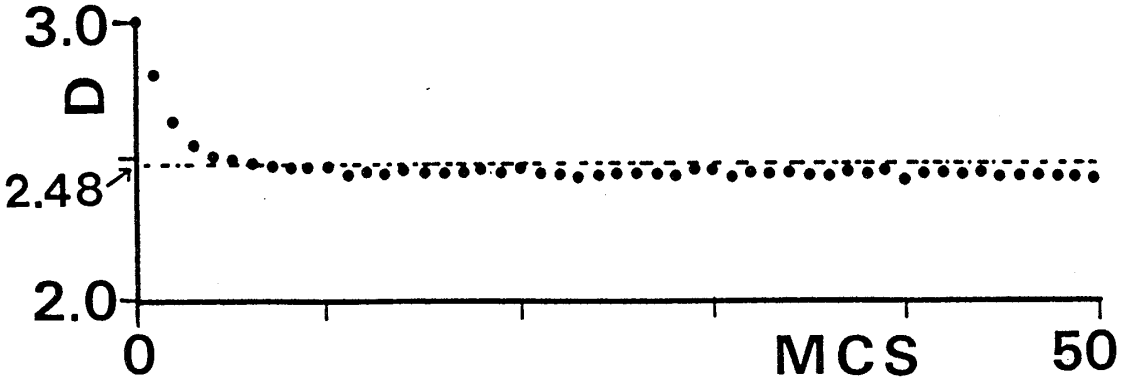

Fig. 1-10 A plot similar to Fig. 1-7 for the three-dimensional Ising model is shown. The system size is 64^2 and the scale used in the coarse graining is $b = 3$.

the system at the temperature closer to the critical point is shown Fig. 1-12. The behavior of the fractal dimensionality is more sensitive to the temperature in the three-dimensional case than in the two-dimensional case.

1.3.3 Four-Dimensional Case

In this case, only the definition (1-3) is tested. The expected value of D is $d = 4$ in the ferromagnetic phase, $d/2 = 2$ for the paramagnetic phase and $d - \beta/\nu = 3$ at the critical point. The critical point is estimated to be about $K = 0.15$ by the high-temperature expansion method[1-39]. As shown in Fig. 1-13, the expected behavior is observed.

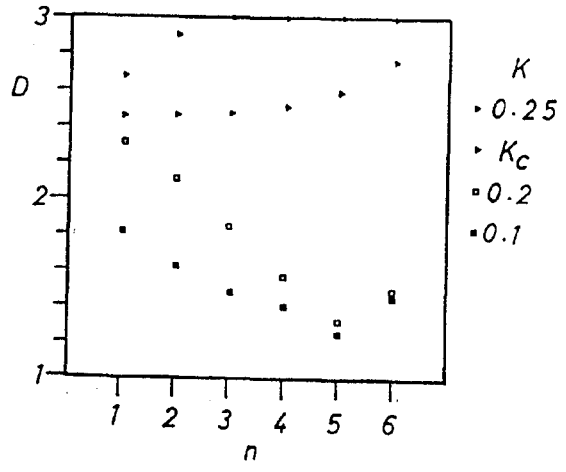

Fig. 1-11
The behavior of $D_n(2)$ for three dimensional 64^3 system is shown.

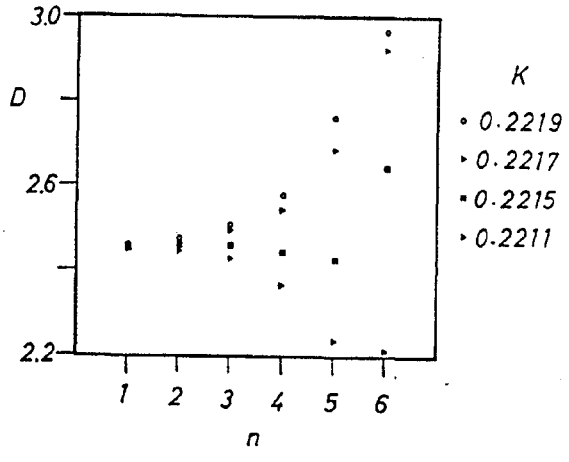

Fig. 1-12
The behavior of $D_n(2)$ for three dimensional 64^3 system around the critical point is shown.

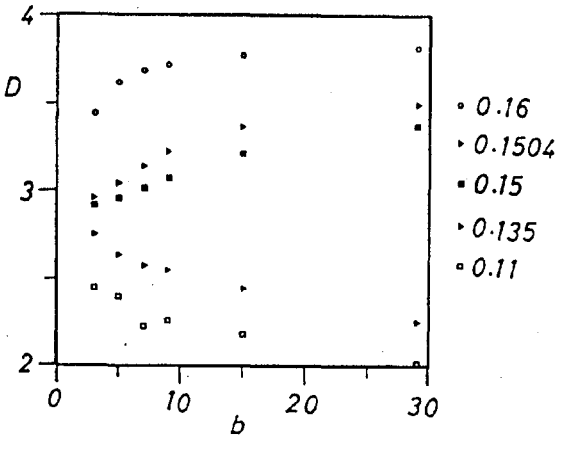

Fig. 1-13
The D for four-dimensional 30^4 system is plotted. The critical temperature is about $K = 0.15$.

1.4 Relation to Scaling of the Distribution Function

Binder[1-30] has studied the Ising model block distribution functions. He found

that the magnetization distribution function $P_L(M)$ in finite blocks of linear dimension L satisfies the scaling relation,

$$P_L(M) = L^{-D} f(L^{-D} M), \qquad D = d - \beta/\nu. \tag{1-6}$$

The relation to this scaling and our fractal picture is studied in this section.

At first, we consider the general situation where any quantity A_L, which depends on the size parameter L, obeys the distribution function $P_L(A_L)$ which shows scaling behavior like

$$P_L(A_L) = L^{-D} \tilde{P}(A_L/L^D), \tag{1-7}$$

where $P(x)$ is normalized so as to fulfill $\int P(x)\,dx = 1$. Then the expected fractal dimensionality is calculated to be D as

$$< D >_P = \int dx \int dy \frac{\log(x/y)}{\log b} P_{bL}(y) P_L(x) = D \tag{1-8}$$

Therefore we cannot distinguish between the true fractalness and such case. Then the variance of D is estimated as

$$< (\Delta D)^2 >_P = \frac{2}{(\log b)^2} < (\Delta \log x)^2 >_{\tilde{P}} \tag{1-9}.$$

To observe its magnitude, the gaussian distribution is considered as an example. In the case of following distribution,

$$P_L(S) = \frac{2}{\sqrt{2\pi\sigma^2}} e^{-S^2/(2\sigma^2)} \qquad S > 0, \tag{1-10}$$

where $\sigma = L^D$. Then we have

$$\sqrt{< (\Delta D)^2 >} = \frac{\pi}{2 \log b} \tag{1-11}.$$

If the factor b is three, this value of $\sqrt{< \Delta D)^2 >}$ is 1.43, namely of order one.

In our results, the distribution function of the block magnetization by Binder is used to examine the deviation of the dimensionality D. The calculated $\sqrt{< \Delta D)^2 >}$ is equal to 1.07 for scale factor three.

The observed $\sqrt{< \Delta D)^2 >}$ estimated from Fig. 1-14 is 0.02. This value is very small compared with the previous value 1.07.

The value 1.07 is a naive estimation. For example the configuration which has a large value of magnetization usually has also a large value of magnetization after scale transformation. This effect is not considered.

Anyway, our fractality is not a trivial result by the scaling of block distribution function.

Whether the deviation of D shown in Fig. 1-14 vanishes or not as the system size becomes infinite is not yet tested. Multi-fractal analysis[1-40] may be useful for detailed analysis of the configuration.

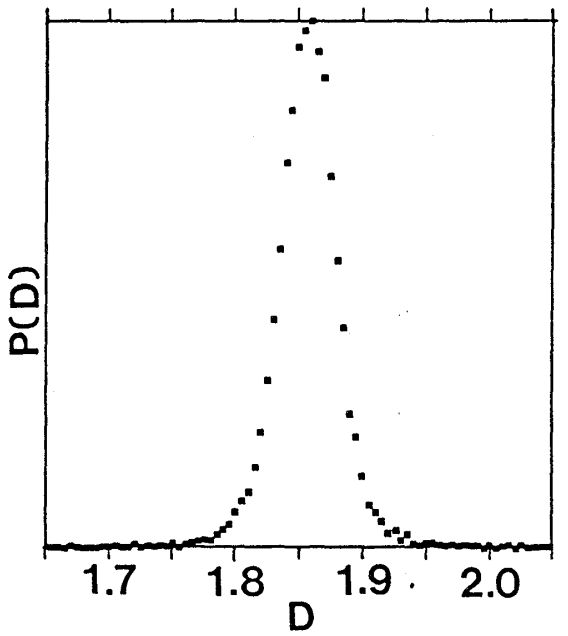

Fig. 1-14
The observed distribution of $D(3)$ for two dimensional 64^2 system. The deviation of D is very small compared with naive estimation from scaled block magnetization distribution function.

1.5 Discussions

Cambier and Nauenberg[1-41] recently obtained $D_R = 1.9 \pm 0.06$ and 2.30 ± 0.05 for two- and three-dimensional cases by analyzing clusters in the configurations. Their definition of the dimensionality D is

$$n \sim R^D,$$

where R and n are the linear dimensionality and the number of spins in one cluster. From their value of D_R for the three-dimensional case, they concluded that Suzuki's conjecture[1-22] was not correct in the three-dimensional case. Our value D is, however, consistent with the known values of critical exponents. Their definition of the D_R may not be appropriate for the purpose to confirm Suzuki's conjecture.[1-22]

Our argument yields automatically the hyperscaling relation $d\nu = 2\beta + \gamma$. Therefore in the Ising case, its validity must be limited to the dimensions less than or equal to four. The four-dimensional case is marginal. The hyperscaling is the result of our fractal nature of the configurations and the finite-size scaling. If we assume that our fractal picture is correct for dimensions higher than four, the finite-size scaling exponent ν' which scales the system-size L and temperature $t = T - T_c$ like L/t must satisfy $d\nu' = 2\beta + \gamma = 2$. Therefore $\nu' = 2/d$. This is also predicted by other authors[1-27] and confirmed for the five-dimensional case by Binder[1-26].

In this chapter, we have established the relation between the fractal and critical phenomena. We have confirmed an extended version of Suzuki's conjecture in the case of two-, three- and four-dimensional square and simple cubic lattice Ising models.

1. Appendix A

D(b) of the random percolation

The symbol Λ denotes the d-dimensional hypercubic lattice of linear size b which is any positive integer:

$$\Lambda = \{x = (x_1, x_2, \ldots, x_n) \in Z^d; \quad 1 \leq x_i \leq b \quad for \quad i = 1, 2, \ldots, n\}.$$

A random variable $X_x \in \{+1, -1\}$ is defined at every $x \in \Lambda$. The probability of $X_x = +1$ is p and that of $X_x = -1$ is $q = 1 - p$ for all $x \in \Lambda$.

The expectation values of $M_b = \sum_{x \in \Lambda} X_x$ and $M_b^{sc} = \mathrm{sgn}(M_b)$, where $\mathrm{sgn}(x)$ denotes the sign of x, are necessary to estimate $D(b)$. The quantities

$$< M_b > \qquad and \qquad < (\Delta M_b)^2 > = < (M_b - < M_b >)^2 >,$$

are calculated easily and the results are

$$< M_b^2 > = N(p - q) \qquad and \qquad < (\Delta M_b)^2 > = 4pqN,$$

where $N = b^d$.

The central limit theorem implies that the distribution of

$$S = \frac{M_b - < M_b >}{\sqrt{< (\Delta M_b)^2 >}}$$

approaches the Gaussian distribution with mean value $\mu = 0$ and standard deviation $\sigma = 1$ when b approaches infinity. If b is large, we can use this Gaussian distribution and obtain

$$< M_b^{sc} > = < \mathrm{sgn}(M_b) > = 2 \ \mathrm{erf}\left(- \frac{< m_b >}{\sqrt{< (\Delta M_b)^2 >}} \right) - 1,$$

where

$$\mathrm{erf}(x) = \frac{1}{\sqrt{2\pi}} \int_x^\infty e^{-x^2/2} \, dx.$$

Therefore we arrive at

$$D(b) = \lim_{p \to \frac{1}{2}} \frac{\log \frac{< M_b >}{< M_b^{sc} >}}{\log b} = \frac{d}{2} + \frac{\log \frac{1}{\sqrt{2\pi}}}{\log b} \quad \to \quad \frac{d}{2}. \qquad (1 - A - 1)$$

1. Appendix B

The Art of Monte Carlo Simulations on Vector Processors

The appearance of a vector processor, or a super-computer, recommend us to adopt new algorithms which are suited for vector processors. The traditional theory of numerical complexity, which treats the total number of arithmetical operations, is not useful, because the power of vector processors depends largely on the vectorizability of the algorithms.

A vector processor is, in a sense, a special purpose computer for the matrix operation. Therefore the Monte Carlo simulation on the vector processor requires some technique which is not effective in a universal purpose processor, or a scalar processor. Such techniques are introduced shortly in this appendix.

An effective multispin coding technique[1-42)~1-43)] is developed recently by Bhanot, Duke and Salvador[1-42,1-43)]. This works not only for a vector processor but also for a scalar one. This method is also introduced.

Using these techniques, our program can treat 2 M, 120 M and 847 M spins per second on HITAC M260 (scalar), HITAC S810 (vector) and HITAC S820 (vector) for the three-dimensional ferromagnetic Ising model. This 847 M updates per second is the fastest Monte Carlo simulator in the world up to now.

(1) Multi-Spin Coding of the Same Site of the Different systems

Ising spin takes only two states, up or down, so one Ising spin have one-bit information. Therefore we can store the state in only one bit of computer memory. This spin coding method is called the multi-spin coding technique, because usually we use integer variables in FORTRAN to store the spins and assign many spins for one variable. The multi-spin coding saves memory and data transfer time. Logical operations are used to treat spins.

The traditional multi-spin coding[1-42,1-43)] codes some spins of the same system for each variable. Bhanot, Duke and Salvador[1-44,1-45)] proposed a new algorithm which saves the effort of random-number generation very much. They proposed to code the same spins at different temperatures or fields systems in one word (Fig. 1-A-1). The merit of their coding is that this coding requires only one random number for spins in one word.

(2) Vectorizable Spin Flip Dynamics

The sequential-flip dynamics and random-flip dynamics are not suited for vectorization. The sublattice-flip dynamics is easily vectorizable.

Spins are divided into some sets (sublattices) so that the spins belonging to one set may be treated independently and simultaneously. An example of sublattices is shown in Fig. 1-A-2.

(3) Vectorization of Random Number Generation

To generate random numbers is the most important ingredient in Monte Carlo calculations. Therefore one has to be careful in using it. Two kind of algorithms[1-40)] are familiar to generate random numbers. One is the linear congruential sequence[1-40)] and the other is the Tausworthe sequence[1-47)~1-50)]. The nature and vectorization technique are described in the following.

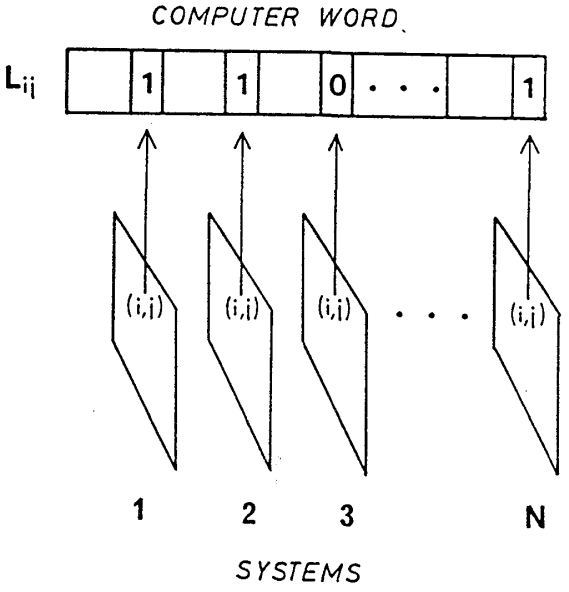

Fig. 1-A-1
The multi spin coding of the same spin of different two-dimensional systems is shown. Each plane denotes the system whose size is the same but system parameters like temperature and field are different.

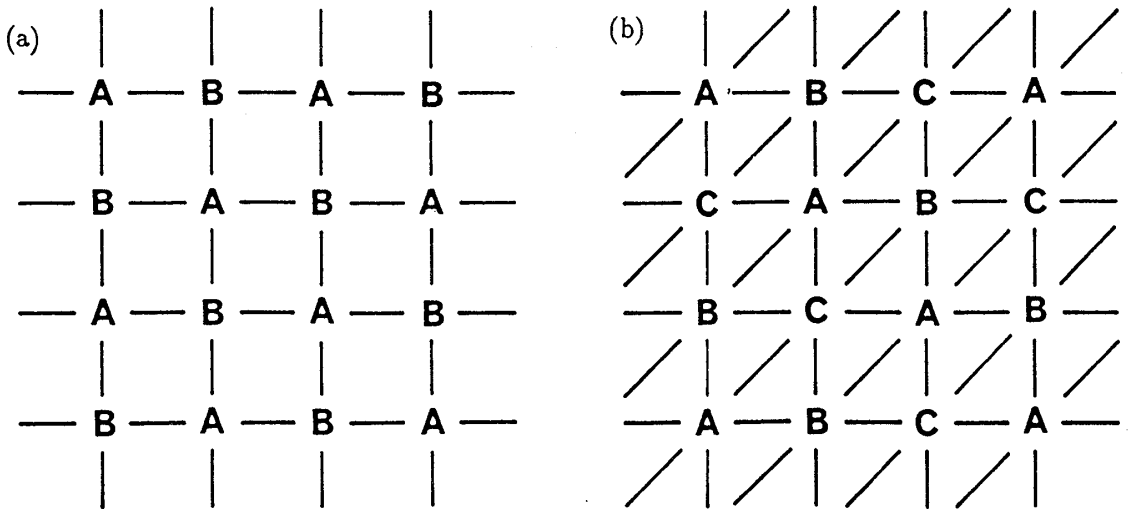

Fig. 1-A-2 Examples of the sublattice division. (a) is the square lattice and (b) is the triangular lattice.

I. Linear Congruential Sequence

This sequence is generated by the following recursion formula

$$R_{k+1} \equiv nR_k + c \pmod{m}. \qquad (1-A-2)$$

The ordinary values of c, m and n are 0, 2^{31} and 5^{11}, respectively. The modulo 2^{31} calculation is easily realized by integer operation. Therefore the recursion formula is

$$R_{K+1} \equiv 5^{11}R_n \pmod{2^{31}}. \qquad (1-A-3)$$

The period p of this sequence is obtained by solving the equation

$$R_0 \equiv 5^{11p} R_0 \pmod{2^{31}}. \qquad (1-A-4)$$

This equation can be easily solved by using index. If R_0 is odd, the p is 2^{29}. If R_0 is $2^t r$ where r is odd, p is 2^{29-t}. Therefore the period of this method is short and this method is not suited for large scale simulations. For example, the period is exhausted only 2048 MCS for a 64^3 system.

The vectorization of this method is accomplished by preparing a special number N_i which is defined by

$$N_i \equiv 5^{11i} \pmod{2^{31}}. \qquad (1-A-5)$$

The sequence

$$R_{n(i+1)+m} \equiv N_i R_{ni+m} \pmod{2^{31}}$$

generates random number in every i distance. Then this enables to realize up to the length-i vectorization.

II. Tausworthe Sequence

This method uses the bit sequence defined by

$$b_k \equiv b_{k-m} + b_{k-n} \pmod{2}, \qquad (1-A-6)$$

where the n and m $(n > m)$ are selected so as the polynomial $x^n + x^m + 1$ may be primitive. An example of them is $n = 250$ and $m = 103$. Other pairs (n, m) are listed by Zierler and Brillhart[1-48,1-49]. The period of this sequence is $2^n - 1$. We can use this sequence as random numbers. The nature of this sequence is studied by Tausworthe. The period of this sequence is large enough for ordinary scale simulations, although we have to use large n for very large scale simulations.

This sequence is realized by logical operation in a computer like

$$b_k = b_{k-n} \oplus b_{k-m}, \qquad (1-A-7)$$

where $\oplus$ denotes exclusive-OR.

To vectorize this sequence, the following formula is useful:

$$(a \oplus b) \oplus (b \oplus c) = a \oplus c. \qquad (1-A-8)$$

The sequence $\{b_k\}$ is rewritten like

$$b_k = b_{k-2^l n} \oplus b_{k-2^l m} \quad for \quad l = 0, 1, 2, \ldots. \qquad (1-A-9)$$

This formula enables us vectorization up to the length-$2^l m$.

第２章　要旨

動的臨界指数ｚの値については、およそ２ということ以外にははっきりとは分っていなかった。２次元イジングモデルについての最近の研究は２．１付近に落着いているようである。本章では、２次元イジングモデルについてｚを評価した。臨界点で異なる大きさの系の相関時間をモンテカルロシミュレーションにより計算し、有限サイズスケーリングを仮定して求めた。その結果は

$$z = 2.132 \pm 0.008$$

である。この結果は、Ｒａｃｚ とＣｏｌｌｉｎｓによる予想値１７／８を支持する。

このシミュレーションは専用計算機ｍ－ＴＩＳにより行なった。この計算機は、イジングスピンのモンテカルロシミュレーションを高速で行なうために我々が設計、製作したものである。ホストコンピュータから転送された系の局所情報に基づきシミュレーションを行なって、結果をホストに返すというものである。システムは、ホストコンピュータ、クロック発生器、局所情報レジスタ、スピンフリッパ、乱数発生器および磁化測定器からなる。ホストコンピュータが十分に速ければ、一秒間に５Ｍスピンを扱う能力を持つ。現在のホストＥＰＳＯＮ　ＰＣ２８６の場合、三次元強磁性イジングモデルで一秒間に約２Ｍスピン扱える。appendixにシステムの概要を示す。

2-1. Dynamical Critical Phenomena

Since Suzuki and Kubo[2-1] formulated the mean-field theory of the kinetic Ising model and the fluctuation-dissipation theorem for stochastic dynamics, many studies[2-2)~2-7] have been made about the dynamical exponent z of the kinetic Ising model. The former results of z is summarized in Ref. 2-7). The estimated values of z vary from 1.8 to 2.3 and not yet settled.

Recently, special-purpose computers[2-8,2-9] turn out to be very powerful tools for computational physics, especially for spin systems. Taiji, Ito and Suzuki designed and constructed a special-purpose computer system for Ising spin systems named m- TIS, which represents the mega spin model of Tokyo university Ising Spin machine. This m-TIS can treat some millions of spins per second when it is connected to an appropriate host computer. The present host computer is EPSON PC-286 which is a compatible machine of NEC PC-9800 series and has CPU 80286 with clock $10MHz$. The detailed report of this system is described in the appendix of this chapter.

In this chapter, the relaxation time of the two-dimensional kinetic Ising model is studied by Monte Carlo calculation using m-TIS and the dynamical critical exponent z is estimated.

The stochastic dynamics of the Ising model is reviewed shortly following Suzuki and Kubo[2-1]. In the case of continuous time, the stochastic time evolution of the system is represented by

$$\frac{dP(\sigma,t)}{dt} = \Gamma P(\sigma,t), \qquad (2-1)$$

where $P(\sigma,t)$ is the probability distribution over the configuration space $\Omega = \sigma$, $\sigma_j = \pm 1$ at time t. The Γ is the operator defined by

$$\Gamma f(\sigma) = (F_j - 1)\, w_j(\sigma) f(\sigma), \qquad (2-2)$$

where F_j denotes the operator which flips the j-th spin σ_j. Therefore its action is represented by

$$F_j f(\ldots \sigma_j \ldots) = f(\ldots -\sigma_j \ldots). \qquad (2-3)$$

The transition probability $w_j(\sigma)$ is determined so as to fulfill the detailed balance condition,

$$w_j(\sigma) P_{eq}(\sigma) = F_j w_j(\sigma) P_{eq}(\sigma), \qquad (2-4)$$

where $P_{eq}(\sigma)$ denotes the equilibrium distribution, and for this stochastic process to have the ergodic property.

When one tries Monte Carlo calculations, it is desirable to clarify the dynamical nature of his dynamics so as to confirm that the system reaches to equilibrium and to estimate the errors correctly. Therefore the study of dynamical properties is important to get exact result by Monte Carlo method.

2.2. Estimation of the Dynamical Critical Exponent

Our Monte Carlo dynamics is described in the following, namely, we treat the two-dimensional square-lattice Ising model with troidal boundary condition and the lattice point is denoted as (i,j) which means i-th row and j-th column lattice

point. The time is discretized and spin flip is tried sequentially from $(1,1)$-site to $(1,n)$-site and then from $(2,1)$-site to $(2,n)$-site and so on. Therefore the time evolution equation is rewritten as

$$P(\sigma, t+1) = \Lambda P(\sigma, t),$$

where Λ is defined by

$$\Lambda = \Lambda_{(n,n)} \cdots \Lambda_{(n,1)}\ \Lambda_{(n-1,n)} \cdots \Lambda_{(2,n)} \cdots \Lambda_{(2,1)}\ \Lambda_{(1,n)} \cdots \Lambda_{(1,1)} \qquad (2-5)$$

and

$$\Lambda_{(i,j)} f(\sigma) = (F_{(i,j)} - 1) W_{(i,j)}(\sigma) f(\sigma). \qquad (2-6)$$

Our flip algorithm is the Metropolis method. Therefore $W_{(i,j)}$ is defined by

$$W_{(i,j)} = min\{1, \exp(2\beta E_{(i,j)})\}, \qquad (2-7)$$

where

$$E_{(i,j)} = -J \sum_{(k,l):n.n.of(i,j)} \sigma_{(k,l)}.$$

We have studied the correlation time of the magnetization. We define the magnetization-magnetization time correlation function $C(\tau)$ by

$$C(\tau) = < M(t)M(t+\tau) > = \lim_{N\to\infty} \frac{1}{N} \sum_{t=0}^{N-1} M(t)M(t+\tau), \qquad (2-8)$$

where $M(t)$ is the magnetization of the system at time t.It is easily shown that $C(t)$ shows multi-exponential decay. The longest decay time is called the correlation time and denoted by ξ . This ξ is finite, because the time evolution operator Λ has only one eigenvalue 1 corresponding to the equilibrium state, and the equilibrium state has even property for spin global inversion operation although magnetization has odd property. This correlation time diverges around the critical temperature as

$$\xi_t \sim \varepsilon^{-z}, \qquad (2-9)$$

where

$$\varepsilon = T - T_c.$$

This is the critical slowing down phenomenon. We have estimated the value of z using the finite-size scaling method. If we assume the finite-size scaling, the correlation time of finite systems whose linear size is L at critical temperature behaves like

$$\xi_t \sim L^z \qquad (at \quad T = T_c). \qquad (2-10)$$

We investigated the correlation time of finite systems at the critical point by the Monte Carlo method using m-TIS. The system sizes we have used are $16^2 \sim 144^2$. For each system size, about one thousand times of correlation time ξ_t Monte Carlo steps are tried and the values of magnetizations are recorded to diskettes. Then the sequence of the values of magnetizations is divided into about

5 pieces and magnetization-magnetization correlations $C(t)$ are calculated from each piece. The values of $C(t)$ are calculated from each pieces following equation (2-8) and the errors of $C(t)$ are estimated from the deviations of the values of $C(t)$ of each pieces.

The χ^2 fitting is tried for the obtained values of $\log C(t)$ by assuming that the distributions of the errors of $\log C(t)$ is Gaussian. Of course, this assumption is not correct. The distributions of the errors of $\log C(t)$ are not Gaussian. However the obtained data must not be so much different from the true estimation and the difference between the result of the χ^2 fitting and the result of true fit must be within the error. An example of the obtained values of $C(t)$ and fitted curve of $C(t)$ is given in Fig. 2-1.

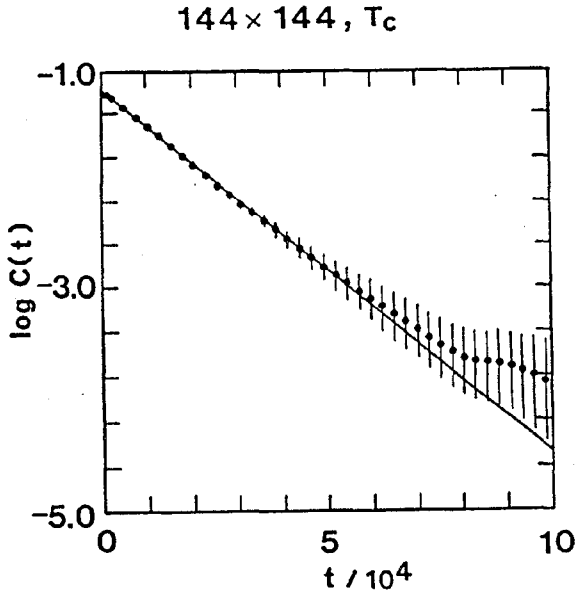

Figure 2-1
The obtained values of $C(t)$ with error bars are plotted as an example. The system is 144^2. The fitted curve is
$\log C(t) = -3.288 \times 10^{-5}(\pm 0.074 \times 10^{-5})t + 0.3078(\pm 0.005)$.

The values of the correlation time is given in Table 2-1.

L	ξ_t	error of ξ_t	Monte Carlo Steps $\times 10^6$
16	285.6	4.3	3
32	1258	28	6
48	2874	44	10
64	5380	140	10
80	8810	67	15
96	12300	280	10
112	18380	270	20
128	23950	480	18
144	30410	680	40

Table 2-1 Magnetization-magnetization correlation time of two dimensional Ising model for L^2 system at critical point is listed. The dynamics is explained in the text.

Figure 2-2 is the plot of obtained values of correlation time for each system size. From this plot, one can observe that the time correlation behaves like L^z from the 16^2- to 144^2-systems. We applied the χ^2 fitting to the values of $\log L$ and $\log \xi_t$ and estimated the values of z, although the errors are also not Gaussian. The obtained value of z is 2.132 ± 0.008.

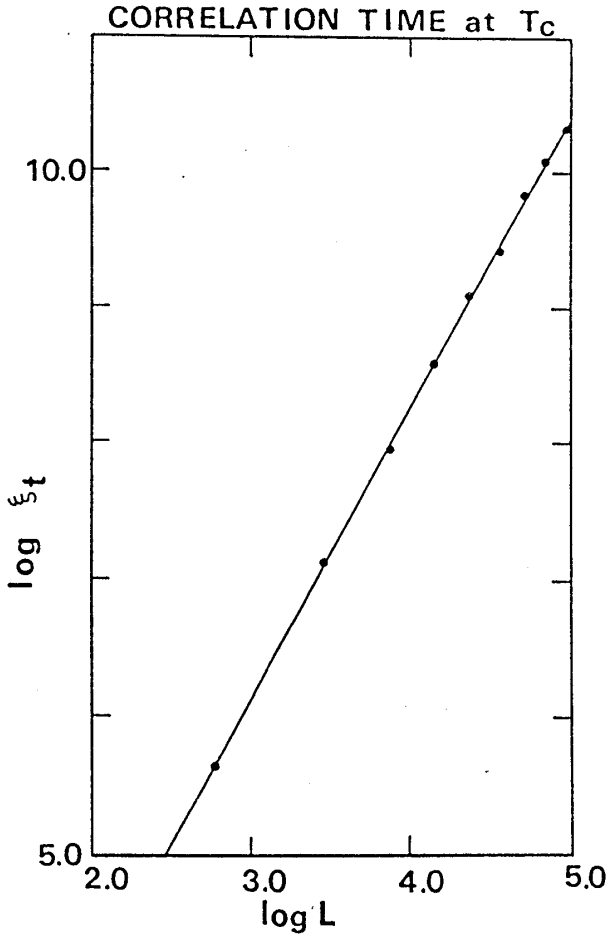

Figure 2-2
The obtained values of correlation times are plotted. The error bars are smaller than the dots. The line represents
$\log \xi_t = 2.132(\pm 0.008) \log L - 0.265(\pm 0.003)$,
which is obtained by χ^2 fitting.
Therefore the estimated values of z is 2.132 ± 0.008.

2-3. Discussions

The obtained value of z supports the conjecture by Rácz and Collins [2-3] that the values of z is $17/8 = 2.125$. They proposed this conjecture from their result $z = 2.125 \pm 0.01$ by high-temperature expansions. If the value of z is really $17/8$, there must be some theoretical explanation for this z to be such a neat rational number.

There are another view point[2-10] about the dependence of ξ_t, which said that ξ_t behaves like $\varepsilon^2(\log \varepsilon)^x$. It is difficult to distinguish the difference between this form and power dependence. From our result the value of x is found to be about 0.49 ± 0.03. This value of x does not agree with the Domany's conjecture[2-10] that this values of x is equal to 1. The difficulty of this Domany's conjecture is also pointed out by Kalle[2-5].

2. Appendix

Special-Purpose Computer System, m-TIS

The special-purpose processor for Ising spin systems which is named the m-TIS, mega-spin model of Tokyo University Ising Spin machine, is designed and constructed to study the spin systems by the Monte Carlo method. The m-TIS can treat several millions of Ising spins per second when it is connected to an appropriate host computer and the maximum ability is about ten millions per second. This machine can treat the Ising spin systems which have one translation invariant direction in the lattice and which have local Hamiltonians including less than 13 spins, for example, Ising models with external field, $\pm J$ spin glasses and $\pm H$ random field models. This machine is used for the study in this appendix.

(1) INTRODUCTION

Lattice systems are actively studied as the models of magnetic materials and field theory using the Monte Carlo method[2-11)~2-14)]. In this field, the use of universal-purpose computers including super-computers turned out not to be the best selection[2-8,2-9)]. Condon and Ogielski[2-15)] in Bell Laboratories made special-purpose systems for Ising spins. Using this system, Ogielski and Morgenstern[2-16)] and Ogielski[2-17,2-18)] have studied the three-dimensional $\pm J$ Ising spin glass and discovered the existence of the spin-glass transition in three-dimensional lattices. There are other two special-purpose machines for Ising spin systems made by Hoogland and his collaborators[2-19)] in Delft and by Pearson and his collaborators[2-20)] in Santa Barbara. The Delft group has studied the finite-size scaling in three dimensions[2-21)], two-dimensional models with multiple spin interactions[2-22)], the Ising model with crossing bonds[2-23)], random number sequences and cellular automata[2-24)]. The Santa Barbara group has studied the three-dimensional Ising model using the finite-size scaling[2-25,2-26)] and its dynamics[2-27)]. Special-purpose computers for other models have also been constructed[2-8,2-9)]. The most remarkable machine is the GF11 by Beetem, Denneau and Weingarten.[2-28)] The GF11 is the parallel-processor machine designed for lattice QCD calculation.

All the Ising machines constructed previously have the memories for spins in a special processor or share them with the host computer. The Monte Carlo dynamics is, roughly speaking, determined by the hardware of the processor, but the recent development of micro computers enables us to introduce another architecture. Our machine m-TIS works, in a sense, as subroutines of spin flipping processes. When information on configuration and randomness is transferred to the m-TIS from the host computer, the m-TIS returns the results of its simulations. The configuration of the system is stored in the memories of the host computer. Therefore the flip sequence can be partially controlled by the software. This machine is cheaper and easier to make than the previous machines because of this separation of the configuration memory and progress in integrated-circuits technology. The detail of this system is presented in the following sections.

(2) CONSTRUCTION OF THE m-TIS

We use an EPSON PC-286 model 0 as a host computer. It is compatible with the NEC PC-98 series personal computer. Our machine m-TIS is designed as a 16-bit bus oriented system because the host has a 16-bit bus.

Figure 2-A-1 shows an example of spin coding. We consider binary one as up spin (+1) and zero as down spin (−1). Spins are close- packed in a word. (A word means 16 bits.) A sequence of bits reflects that of spins; the next spin of bit 0 is bit 1, the next spin of bit 1 is bit 2 and so on. Therefore the linear dimension of a lattice must be a multiple of 16 at least in one direction. The machine flips spins sequentially from bit 0 to bit 15. Condon and Ogielski packed a lattice into "spin words"which are placed on "word lattice.[2−15]" Our packing has the following advantages compared with theirs.

(1) It is easy to display a configuration of spins in a bit map screen.
(2) We can easily change the linear dimension of a lattice by modifying a software. No modification of the hardware is necessary.
(3) The hardware is simple.

A block diagram of the system is shown in Fig. 2-A-2. The system is composed from six parts: the host microcomputer, the clock generator, the local information registers, the spin flipper, the random number generator and the magnetization counter.

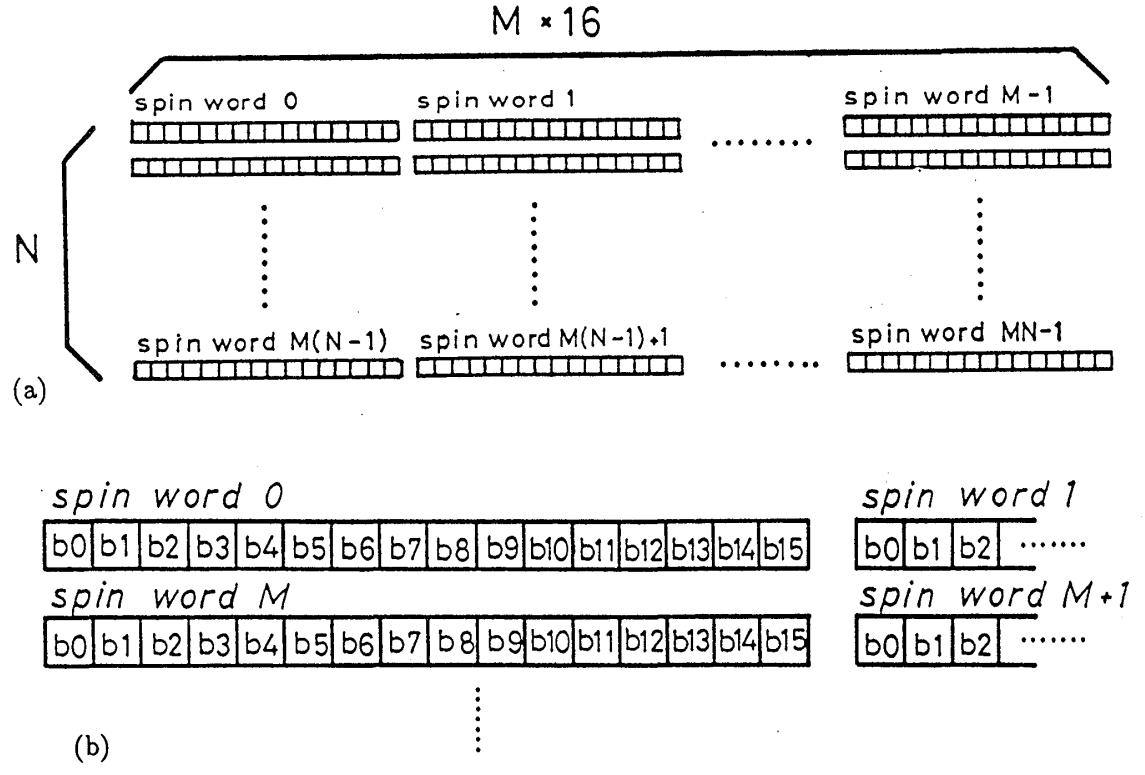

Fig 2-A-1 (a) An example of spin coding in the case of the two- dimensional square lattice $(16M)xN$. Each long box denotes one word, which we call a "spin word." Each small box denotes a spin (a bit) and the physical lattice point.
(b) Magnified picture of the upper left part of (a). It shows the sequence of spins in spin words. Symbols $b0 - b15$ represent the bit order in word, $b0$ is the LSB (least significant bit) and $b15$ is the MSB (most significant bit).

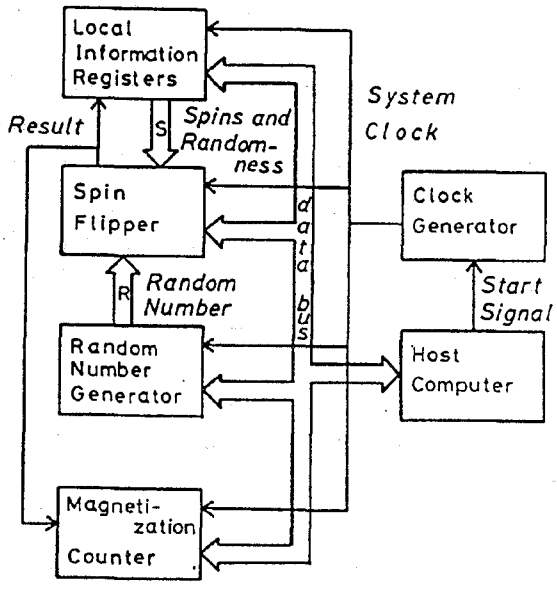

Fig. 2-A-2
Block diagram showing the entire system of the m-TIS.

i) The clock generator

It generates 16 clock pulses called "system clock"when it receives a start signal from the host computer. An interval between pulses is $200ns$ at present. The system works synchronously with this clock and flips one spin per one pulse. Therefore, It can flip 5×10^6 spins per second at its best. This interval can be decreased up to $100ns$ or 10×10^6 spins per second if we use the RAM of access-time $35ns$ for the Boltzmann factor memories of the spin flipper.

ii) The random number generator

It generates a 16-bit random number synchronously with the system clock. A binary random number sequence is generated by the two-bit feedback shift register method or Tausworthe method[2-29)~2-32)], which determines the next bit by

$$R_n \equiv R_{n-33} + R_{n-68} \pmod 2. \qquad (2-A-1)$$

We use these serial 16 bits as a random number. The hardware generates 16 bits simultaneously as explained in Fig. 2-A-3. It is composed of 16-bit parallel four- or five-stage shift registers and 16 exclusive-or gates.

These 16-bit random numbers are sufficient for ordinary simulations. If necessary, more accurate random numbers can be used by replacing the random number generator and Boltzmann factor RAMs.

iii) The local information registers

They store information on resultant spins, spins to be treated, neighbor spins and randomness. They send it to the spin flipper and receive the result synchronously with the system clock. They consist of a 64-bit, a 20-bit and eight 16-bit shift registers. The local information registers have input latches, so that we can set the next data to the shift registers while simulating.

Figure 2-A-4 shows the composition of the local information registers. They consist of a 64-bit, a 20-bit and eight 16-bit shift registers. The 64-bit register

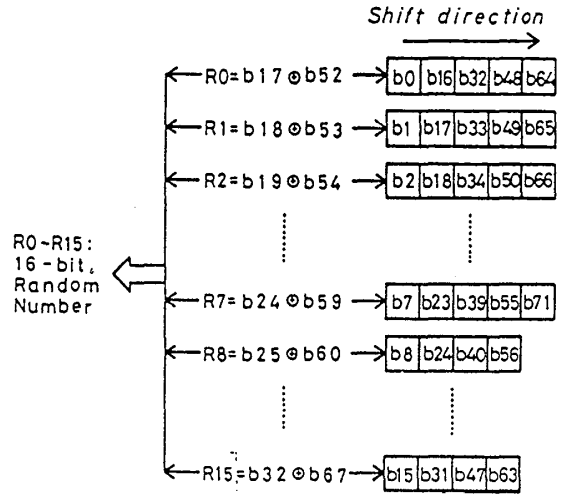

Fig. 2-A-3

Construction of the random number generator. The rows of boxes represents shift registers and each box is considered as one bit. When the system clock goes up, random numbers $R0 - R15$ are written to $b0 - b15$, respectively, and the registers are shifted. Then a new 16-bit random number $R0 - R15$ is generated.

stores spins to flip. It works as 16-, 32-, 48- or 64-bit ring shift register. This structure makes simulations faster not only for large systems but also for small systems. The 20-bit register is used for the Ising spin glass to store bond randomness of the direction in which the simulation is progressing or is used for the two-dimensional triangular lattice to store up (or down) nearest neighbor spins. Because two bits of this register are connected with the spin flipper, it can not compute a six-dimensional hypercubic Ising model. We use the 16-bit registers to store the left,right,up and down nearest neighbor spins and bond randomness, for example, in the case of the three- dimensional Ising spin glass on the cubic lattice. For the two- dimensional triangular lattice, two of these 16-bit registers can be concatenated and work as a 32-bit register to store down (or up) nearest neighbor spins.

No modification of the hardware is necessary to change the structure of a lattice, except for the two-dimensional triangular lattice. In this case, we must move one switch (but it is very easy !).

A linear dimension of the relevant system must be a multiple of 16 in one direction. The maximum size is determined by the memory capacity of a host computer.

iv) The spin flipper

It is the central part of this machine. Figure 2-A-5 shows its block diagram. It receives the information on spins and randomness (totally 13 bits) from the local information registers. Then it generates a probability of flipping a spin as an arbitrary function of thirteen Boolean variables. For this purpose, we use two 8192x8-bit static RAMs (HM6264LP-10, Hitachi) of which address-access-time is $100ns$. The information is connected with the address lines of the S-RAMs and the probability comes from the data lines. This probability is compared with a random number from the random number generator and if the probability is greater than the random number, the spin is flipped. The result is returned to the local information registers.

The flip probabilities are stored in these s-RAMs by the host computer before

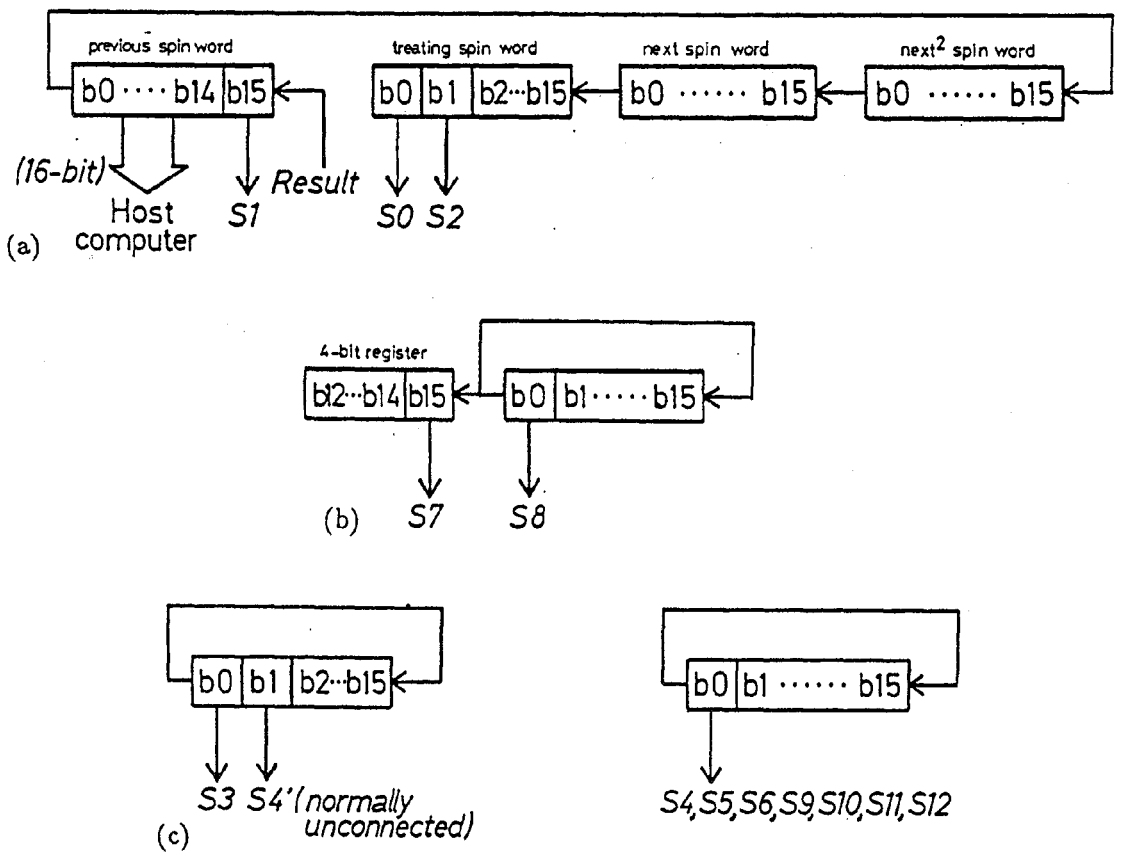

Fig. 2-A-4 Construction of the local information registers. Each long box represents a 16-bit shift register. The information on spins and randomness, $S0 - S12$, is transferred to the spin flipper.

(a) The 64-bit shift register. The variable $S0$ is a now treating spin. The variables $S1$ and $S2$ denote the previous spin and the next spin, respectively.

(b) The 20-bit shift register. We use $S7$ and $S8$ for the Ising spin glass or the two-dimensional triangular lattice.

(c) The 16-bit shift registers. The variables $S3 - S6, S9 - S12$ are independent except for $S3$ and $S4'$. We connect $S4'$ instead of $S4$ while computing spin configurations on the two-dimensional triangular lattice.

beginning a simulation.

v) The magnetization counter

It counts the resultant spins of the spin flipper synchronous with the system clock. We clear it before simulating each Monte Carlo step and read it after the step. Then we obtain the value of magnetization. It is composed of a 20-bit counter. Therefore this counter can treat a system consisting of less than 2^{20} spins.

We summarize a simulation sequence of one Monte Carlo step:

(1) Clear the magnetization counter.
(2) Set information on spins and randomness.
(3) Send start signal to the clock generator. Then the simulation of 16 spins starts.
(4) Set next information and wait the end of simulation.

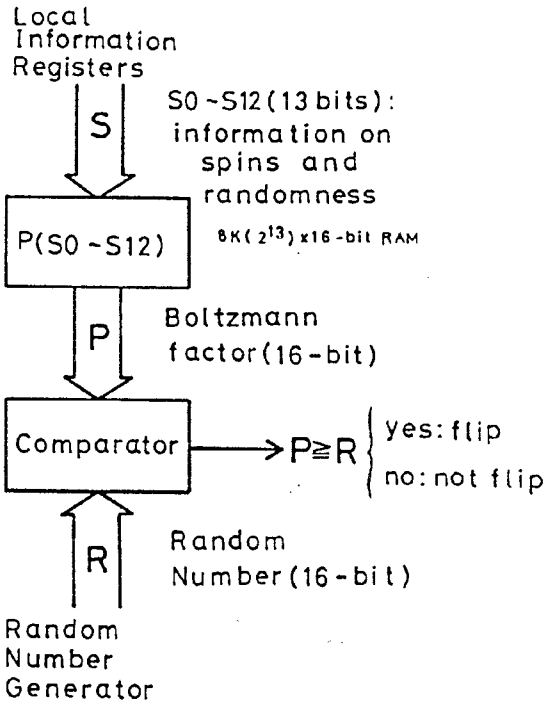

Fig. 2-A-5
Block diagram of the spin flipper. In this figure, P is an arbitrary function of S, which is generated by RAMs.

(5) Get results and store them. Repeat (3)-(5)
(6) Read the magnetization counter and output the result to floppy disks.

Prior to the simulation, the m-TIS must be initialized. The initialization procedures consist of the following two steps.
(1) Set the seed to the random number generator.
(2) Set the Boltzmann factors to the spin flipper.

Figure 2-A-6 shows the photograph of the entire system. The machine consists of about one hundred ICs. They are all commonly used F,AS,ALS TTL ICs and HC-MOS ICs. It was built in five 14.5cm×11.5cm boards. The boards are connected with each other through a mother board with 44pin card edge connectors. The machine and the host computer are connected by 50 line flat cables. The host computer has an interface board to extend a bus. The host controls the machine through an I/O space or a memory space. Now we are using an I/O space for the convenience of programming.

(3) OPERATING ENVIRONMENT

We use Microsoft MS-DOS for development. The routines for simulation are written in 80286 assembly language and the other routines are written in C language. We prepare a "control file "which contains necessary parameters for the simulation such as system sizes, values of temperature and external field, repeat factors, random seeds and output-file names etc. Then the program automatically performs specified simulations and output results to floppy disks. The results are analyzed by other programs. The Hamiltonian of the system is given as a function of local spin variables in the operating program written in C language. Therefore we can change the Hamiltonian by modifying, compiling and linking only one function in C language.

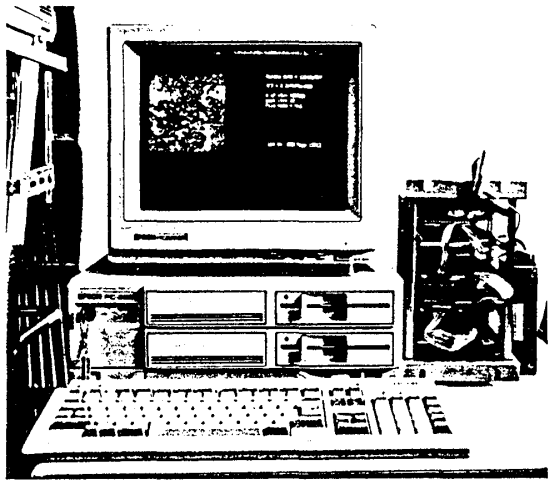

Fig. 2-A-6
Photograph of the entire system of the m-TIS. Our special processor can be seen at the right of the host microcomputer.

(4) SPECIFICATIONS

i) Computable Hamiltonians

As we mentioned before, this machine can simulate Ising spin systems. In the following, we show some examples of computable systems.

(1) Ising spin systems with uniform interactions and external field on one- to five-dimensional cubic and two-dimensional triangular lattices.
(2) $\pm J$-Ising spin glass on one- to three-dimensional cubic lattices.
(3) $\pm H$-random field Ising spin systems on one- to five- dimensional cubic and two-dimensional triangular lattices.
(4) Cellular automata with sequential flip dynamics.

Though the present machine is designed for sequential flip dynamics, a little modification enables us to study simultaneous flip dynamics for the cellular automata.

The local Hamiltonian must be a function of spins to be flipped (1bit) and its neighbor and information on randomness (12 bits in maximum).

Boundary conditions are arbitrary. Periodic boundary condition including the twisted case and fixed one are most easily simulated. Free boundary condition is also simulated using information on bond randomness as the boundary information.

ii) Performance

The performance of the present system is (1) 1.5×10^6 flips per second for the two-dimensional Ising model (square lattice, 256^2) and (2) 1.2×10^6 flips per second for the three-dimensional Ising model (cubic lattice, 64^3), with displaying configurations and recording the values of magnetization to a floppy disk. Without them it can compute 1.2 times faster. The cost- performance ratio is very good compared with universal-purpose computers. This machine is tested by calculating the spontaneous magnetization of the two-dimensional Ising model on the square lattice.

iii) Characteristics

(1) We can observe configurations of spins in real time on CRT screen. It is useful in studying the dynamical natures of models.

(2) Magnetizations are measured with simulation without slowing down.
(3) Low cost. it costs less than 100,000 yen except for a host computer.
(4) You can use a 16-bit personal computer, for example, IBM PC AT, as a host computer.
(5) This machine can treat the Hamiltonian as a function of nearest neighbor spins. Furthermore, the Hamiltonian may depend on other information dependent on site (six bits in the case of the cubic lattice). The flexibility supersedes any other special-purpose machine for Ising spin systems.

(5) SUMMARY AND FUTURE PERSPECTIVES

Our machine is very cheap and has reasonable portability. Its special advantage is its flexibility on Hamiltonians and lattice structures.

This system is already used to study the dynamical critical exponent of the two-dimensional Ising model as described in this chapter.

There is much room for improvement in our machine. We can accelerate it by two modifications. First, we change Boltzmann factor RAMs with much faster ones. Next, we can modify it to store spins and randomness in special memories which the machine can directly access (like the other Ising machines). By these two improvements, it will be able to treat a few ten million spins per second.

第 3 章

鈴木により考案されたＣＡＭ（coherent-anomaly method）は、複数の分子場近似から正しい臨界指数を評価する方法である。ＣＡＭは、近似の度合いによるスケーリング（finite-degree-of-approximation scaling）を導入し、そのスケーリング指数と近似によりえられる指数とから真の臨界指数を評価する方法を与える。現在までに、イジングモデル、スピングラス、パーコレーション等に応用され、有効性が確認されている。

本章は、この方法をハイゼンベルグモデルに応用した結果を示す。分子場近似として、Weiss近似、Bethe近似、constant coupling近似を使った。その結果、ハイゼンベルグモデルの場合にもＣＡＭは機能する様であるが、よい値を得るためにはさらに大きいクラスターでの分子場近似が必要である。

3-1. Introduction to the Coherent-Anomaly Method

The coherent-anomaly method (CAM) proposed by Suzuki[3-1)-3-3)] is powerful to estimate singularities using some series of approximations. A short review of the CAM is given in section 2. This CAM theory is applied successfully to many systems which show critical phenomena so as to estimate the critical points and critical exponents. The systems studied up to now using the CAM theory are Ising models[3-4)~3-8)], spin glasses[3-9)] and random percolation problems[3-9,3-10)]. Recently, the CAM for perturbation expansion methods was also proposed by Suzuki[3-11)] and it is found by Suzuki[3-12)] that the continued fraction is useful to apply the CAM for power series type approximations.

The Ising model is studied in detail by Suzuki, Katori and Hu using the systematic cluster mean-field approximations[3-4)~3-6)] and systematic mean-field transfer-matrix methods[3-7,3-8)]. For the cluster mean-field approximations, the coherent anomalies of the response functions are derived phenomenologically[3-5)] and the convergence of the critical temperature is proven[3-5)]. The obtained values of the critical points and critical exponents of the susceptibility are $K_c = 0.448 \pm 0.008$ and $\gamma = 1.79 \pm 0.12$ for the square lattice and 0.221 ± 0.003 and 1.26 ± 0.07 for the simple cubic lattice[3-5)]. For the systematic mean-field transfer-matrix method, the new scaling relation $\nu^i \eta = \beta$ is obtained from the CAM scaling, where ν^i is the critical exponent of the induced magnetization by an external field on the boundary of the relevant system at the critical point[3 − 8)]. The obtained values of K_c,α,β, γ and δ are 0.4403, 0 (logarithmic divergence), 0.131, 1.749 and 15.1 respectively in two dimensions.

The critical exponent of the non-linear susceptibility χ_2 for $\pm J$-Ising spin glass system on the simple cubic lattice is estimated[3-9)] to be 2.87.

Suzuki[3-9)] has shown how to apply the CAM to the random percolation problems and obtained some results for many types of models. Takayasu and Takayasu[3-10)] obtained very good values from their cluster mean-field calculations of the site problems on hyper-cubic lattices.

In this chapter, the Heisenberg ferromagnet is studied using the CAM theory based on the Weiss, Bethe[3-13)] and constant coupling[3-14)] approximations. The results show that the CAM theory is also powerful for quantum spin systems.

The basic idea of the coherent-anomaly method is given in the following. The mean-field type approximations of magnetic spin systems are considered as examples.

Mean-field type approximations give classical critical exponents irrespective of the dimensionality of the lattice, although the system does not show classical critical values below the upper critical dimensionality of it. Therefore the mean-field theory has not been used to study the system near the critical point. The coherent-anomaly method uses, however, the singular part of mean-field approximations. If the size of a cluster used in an approximation is increased and the effects of the fluctuations are taken into account, this singular part will be modified coherently as the degree of the approximation increases, namely as the difference of the obtained critical temperature from the true one goes to zero. This is the essential point of the CAM theory. The CAM is formulated so as to be able to estimate the true non-classical behavior of the system. Therefore if one calculates

some cluster approximations, the true critical point and the true critical exponents can be estimated approximately with the use of the CAM.

Now we assume that there are two mean-field type approximations, A and B, for a magnetic spin system. The critical points and susceptibilities obtained from these two approximations are denoted by K_c^A, K_c^B, χ^A and χ^B. The susceptibilities diverge at the critical point like

$$\chi^i \sim \bar{\chi}^i \frac{K_c^i}{K_c^i - K} \qquad (K < K_c^i), \quad i = A, B, \tag{3-1}$$

where $\bar{\chi}^A$ and $\bar{\chi}^B$ are some constants. This type of divergence is universal for mean-field-type approximations. Therefore the critical exponent of susceptibility, γ, estimated from these approximations is equal to unity for any models, which is called the classical value. On the other hand, the exact value of γ is 7/4 for the two-dimensional Ising model. The residual divergence, $(K - K_c)^{1-\gamma}$, affects the coefficients $\bar{\chi}^A$ and $\bar{\chi}^B$, respectively. If the obtained critical point is closer to the exact critical point K_c^*, the approximation is better. This implies the relation

$$\bar{\chi}^i \to \infty \qquad \text{as} \qquad K_c^i \to K_c^*. \tag{3-2}$$

The CAM theory assumes the following relation

$$\bar{\chi}^i \sim (K_c^* - K_c^i)^{-\varphi}. \tag{3-3}$$

Therefore the true exponent is estimated by

$$\gamma = 1 - \left[\log \frac{\bar{\chi}^B}{\bar{\chi}^A}\right] / \left[\log \frac{\delta K_c^B}{\delta K_c^A}\right], \tag{3-4}$$

where $\delta K_c^i = K_c^* - K_c^i$.

The spontaneous magnetization of the relevant system emerges in the ordered state near the critical point as

$$m^i \sim \bar{m}^i \sqrt{\frac{K - K_c^i}{K_c^i}} \qquad (K > K_c^i), \quad i = A, B, \tag{3-5}$$

The true exponent of the spontaneous magnetization,β, is estimated by

$$\beta = \frac{1}{2} + \left[\log \frac{\bar{m}^B}{\bar{m}^A}\right] / \left[\log \frac{\delta K_c^B}{\delta K_c^A}\right], \tag{3-6}$$

The difference of the sign in (3-4) and (3-6) originates from the definitions of the critical exponents.

The exact critical point is assumed in eqs. (3-4) and (3-6), but we can dispense with it if we have three or more approximations. The details of the CAM is given in ref. 3-1).

3-2. Mean-Field Theories for the Heisenberg Model

The CAM is applied successfully for many systems as described in section 3-1. The aim of the present paper is to show that the CAM is also useful for quantum spin systems. The isotropic Heisenberg ferromagnet on the simple cubic lattice is used for this purpose. The Hamiltonian of the system is

$$\mathrm{H} = -2J \sum_{|i-j|=1} \vec{S}_i \cdot \vec{S}_j - g\mu_0 \vec{H} \sum_i \vec{S}_i, \qquad \vec{S} = \frac{1}{2}\vec{\sigma}, \tag{3-7}$$

where σ, μ_0 and g are Pauli matrices, Bohr magneton, and the g- factor of spins, respectively.

The high-temperature-expansion analysis[3-15] concludes that the critical point K_c and the critical exponents of the susceptibility and spontaneous magnetization, γ and β are

$$K_c = 0.595 \pm 0.003, \qquad \gamma = 1.43 \pm 0.01 \qquad \text{and} \qquad \beta = 0.385 \pm 0.025, \tag{3-8}$$

where K denotes $J/(k_B T)$.

The Weiss, Bethe and constant coupling approximations are used to estimate the values of β and γ with the CAM. In the following, the results of these approximations for the Heisenberg model with an arbitrary number of the nearest neighbour spins, which is denoted by z, are summarized.

The critical points are denoted by K_c^i, where i denotes Weiss, Bethe and c.c. (i.e. constant coupling). The coefficients of the susceptibility and spontaneous magnetization are defined by

$$\chi^i \sim \bar{\chi}^i \frac{K_c^i}{K_c^i - K} \quad (K < K_c^i), \qquad m^i \sim \bar{m}^i \sqrt{\frac{K - K_c^i}{K_c^i}} \quad (K > K_c^i), \quad i = A, B, \tag{3-9}$$

These are the "skeletonized[3-16]"susceptibility and spontaneous magnetization, or singular part of them.

3-2-1 Weiss Approximation

The Weiss approximation for the Heisenberg model is the same as for the Ising model. The results are

$$K_c^{Weiss} = \frac{2}{z}, \tag{3-10}$$

$$\bar{\chi}^{Weiss} = \frac{g^2 \mu_0^2}{2zJ} \tag{3-11}$$

and

$$\bar{m}^{Weiss} = \frac{\sqrt{3}}{2} g\mu_0. \tag{3-12}$$

3-2-2 Bethe Approximation

The Bethe approximation for the Heisenberg model was obtained by P.R.Weiss[3-13]. We have calculated it again following P.R.Weiss[3-13] and we give,

for the future references, more compact expressions for the coefficients appearing in the results than those in ref. 3-13). In the following, the values of z should be even.

This approximation treats the Hamiltonian,

$$\mathbf{H} = -2J\vec{S}_0 \sum_{i=1}^{z} \vec{S}_i - g\mu_0 H S_0^z - g\mu_0 (H + H_{mf}) \sum_{i=1}^{z} S_i^z, \qquad (3-13)$$

where H and H_{mf} represent, respectively, an external field and the molecular field which is determined by the self-consistency equation. This Hamiltonian is diagonalized exactly and consequently its partition function is derived. It is required that the averaged value of S_0 is equal to that of S_i.

The self-consistency equation which determines the critical point is

$$A = 0, \qquad (3-14)$$

where

$$A = \sum_{k=1}^{2} \sum_{S=0}^{z/2} w(z,S) \left[A_k^0 + \frac{K}{J} A_k^1 \right] e^{-(K/J)A_k} \qquad (3-15)$$

and A_k, $w(z,S)$ and A_k^i are given in (3-A-1),(3-A-2), (3-A-12) and (3-A-13) $\sim$ (3-A-18). The susceptibility is

$$\chi^{Bethe} = \frac{g^2\mu_0^2}{J} \frac{DB}{Z_0 A} \qquad (K < K_c^{Bethe}), \qquad (3-16)$$

where

$$B = \frac{1}{z+1} \frac{K}{J} \sum_{k=1}^{2} \sum_{S=0}^{z/2} w(z,S) B_k^0 e^{-(K/J)A_k}, \qquad (3-17)$$

$$D = \sum_{k=1}^{2} \sum_{S=0}^{z/2} w(z,S) D_k^0 e^{-(K/J)A_k} \qquad (3-18)$$

and

$$Z_0 = \sum_{k=1}^{2} \sum_{S=0}^{z/2} \sum_{m=-M_k}^{M_k} w(z,S) e^{-(K/J)A_k} \qquad (3-19)$$

The coefficients B_k^0, D_k^0 and M_k are given in (3-A-19)$\sim$(3-A-21), (3-A-34)$\sim$(3-A-36) and (3-A-13). Therefore the singular part at the critical point is

$$\chi^{Bethe} \sim \bar{\chi}^{Bethe} \frac{K_c^{Bethe}}{K_c^{Bethe} - K} \qquad (K < K_c^{Bethe}), \qquad (3-20)$$

where

$$\bar{\chi}^{Bethe} = \frac{g^2\mu_0^2}{J} \left[\frac{DB}{Z_0 \frac{\partial A}{\partial K}} \right]_{K=K_c^{Bethe}}. \qquad (3-21)$$

The spontaneous magnetization is

$$m^{Bethe} = \frac{g\mu 0}{z+1}\frac{1}{J}\frac{D}{Z_0}\sqrt{-\frac{K}{C}A} \qquad (K > K_c^{Bethe}), \tag{3-22}$$

where

$$C = \sum_{k=1}^{2}\sum_{S=0}^{z/2} w(z,S)\left[C_k^0 + \frac{K}{J}C_k^1 + \frac{K^2}{J^2}C_k^2 + \frac{K^3}{J^3}C_k^3\right] e^{-(K/J)A_k} \tag{3-23}$$

and the coefficients C are given in (3-A-22)$\sim$ (3-A-33). Near the critical point, the spontaneous magnetization becomes

$$m^{Bethe} \sim \bar{m}^i\sqrt{\frac{K - K_c^{Bethe}}{K_c^{Bethe}}} \qquad (K > K_c^{Bethe}), \tag{3-24}$$

where

$$\bar{m}^{Bethe} = \frac{g\mu_0}{z+1}\frac{1}{J}\left[\frac{D}{Z_0}\sqrt{-\frac{K^3}{C}\frac{\partial A}{\partial K}}\right]_{K=K_c^{Bethe}}. \tag{3-25}$$

3-2-3 Constant Coupling Approximation

The constant coupling approximation is introduced by Kasteleijn and van Kranendonk[3-14]. This method treats the following effective Hamiltonian

$$\mathrm{H} = -2J\vec{S}_i\cdot\vec{S}_j - (mH^z + C)(S_i^z + S_j^z), \tag{3-26}$$

where C is a variational parameter determined by minimizing the free energy. From this approximation, the critical point and the coefficients $\chi^{c.c.}$ and $m^{c.c.}$, are given by

$$K_c^{c.c.} = \frac{1}{2}\log\frac{z}{z-4}, \tag{3-27}$$

$$\bar{\chi}^{c.c.} = \frac{1}{2(z-4)}\frac{g^2\mu_0^2}{J} \tag{3-28}$$

and

$$\bar{m}^{c.c.} = \frac{z}{4(z-1)}g\mu_0\sqrt{\frac{3(z-1)(z-4)}{z-2}\log\frac{z}{z-4}}. \tag{3-29}$$

3-3. Estimation of β and γ by the CAM

The values of critical points and the coefficients of the susceptibility and spontaneous magnetization are given in Table 3-1 for the case of the simple cubic lattice, z=6. Assuming that the exact critical point is the high-temperature-expansion value, 0.595, we can estimate the exponents β and γ from any two of the three,

	Weiss	Bethe	c.c.
K_c	0.33333	0.54005	0.54931
$\bar{\chi}J/(g\mu_0)^2$	0.08333	0.23647	0.25
$\bar{m}/(g\mu_0)$	0.86603	0.87321	0.86114

Table 3-1 The critical temperatures and coefficients obtained from approximate theories are given for the case of the simple cubic lattice, $z = 6$.

	used variable as temperature	Weiss-Bethe	Weiss-c.c.	HTE
γ	K	1.67	1.63	1.43±0.01
	T	1.51	1.49	
β	K	0.495	0.503	0.385±0.025
	T	0.496	0.503	

Table 3-2 Estimated values of the exponents γ and β are listed. Two pairs of the approximations are tried. One is the Weiss and Bethe pair and the other is the Weiss and constant coupling pair. The critical point of the high-temperature-expansion, $K_c = 0.595$, is used as the exact critical point. The difference of the results due to the choice of the variables, K and T, should vanish when the degree of approximation is decreased by using larger clusters.

Weiss, Bethe and constant coupling approximations using eqs. (3-4) and (3-6). The results are listed in Table 3-2.

The estimation of the value of β is more difficult than the value of γ, because the difference between the true value of β and the mean-field value of it is small. Thus the present preliminary results are not so good, but this will be improved when larger clusters are used.

The results of the Weiss and Bethe pair seem to be better, because the anomalies of the spontaneous magnetization emerges correctly. If we make mean-field approximations for larger clusters, more accurate values of the critical point and critical exponents will be obtained. On the other hand, the Weiss and constant coupling pair is not good up to this degree of approximation, because of its incorrect anomalies for spontaneous magnetization. If we try the constant-coupling-like approximation for larger clusters, this difficulty will vanish.

3-4. Concluding Remarks

It is shown that the CAM works successfully for quantum spin systems. The critical phenomena of various quantum systems can be studied by the CAM theory.

3. Appendix

The Coefficients in the Bethe Approximation

$$A_1 = J(S+1) \tag{3-A-1}$$

$$A_2 = -JS \tag{3-A-2}$$

$$b_k = -m \qquad (k=1,2) \tag{3-A-3}$$

$$c_1 = -\frac{m}{2S+1} \tag{3-A-4}$$

$$c_2 = -c_1 \tag{3-A-5}$$

$$d_1 = \frac{1}{4(2S+1)}\left[1 - \frac{4m^2}{(2S+1)^2}\right] \tag{3-A-6}$$

$$d_2 = -d_1 \tag{3-A-7}$$

$$e_1 = \frac{m}{2(2S+1)^3 J^2}\left[1 - \frac{4m^2}{(2S+1)^2}\right] \tag{3-A-8}$$

$$e_2 = -e_1 \tag{3-A-9}$$

$$f_1 = -\frac{1}{16(2S+1)^3 J^3}\left[1 - \frac{24m^2}{(2S+1)^2} + \frac{80m^4}{(2S+1)^4}\right] \tag{3-A-10}$$

$$f_2 = -f_1 \tag{3-A-11}$$

$$w(z,S) = \frac{(2S+1)\ z!}{(z/2-S)!\ (z/2+S+1)!} \tag{3-A-12}$$

$$A_k^0 = \sum_{m=-M_k}^{M_k} (-2d_k), \qquad M_k = \begin{cases} S-1/2 & k=1 \\ S+1/2 & k=2 \end{cases} \tag{3-A-13}$$

$$A_k^1 = \frac{1}{z+1} \sum_{m=-M_k}^{M_k} \left[(b_k+c_k)^2 + z c_k (b_k+c_k)\right] \tag{3-A-14}$$

$$A_1^0 = -\frac{4S(S+1)}{3(2S+1)^2 J} \tag{3-A-15}$$

$$A_2^0 = -A_1^0 \tag{3-A-16}$$

$$A_1^1 = \frac{1}{z+1}\frac{S(S+1)(2S-1)(2S+2+z)}{3(2S+1)} \tag{3-A-17}$$

$$A_2^1 = \frac{1}{z+1}\frac{S(2S-1)(S+1)(2S+3)}{3(2S+1)} \tag{3-A-18}$$

$$B_k^0 = \sum_{m=-M_k}^{M_k} \left[b_k^2 + (z+1) b_k c_k\right] \tag{3-A-19}$$

$$B_1^0 = \frac{S}{6}(2S-1)(2S+z+2) \tag{3-A-20}$$

$$B_2^0 = \frac{1}{6}(S+1)(2S+3)(2S-z) \qquad (3-A-21)$$

$$C_k^0 = \sum_{m=-M_k}^{M_k} (-4f_k) \qquad (3-A-22)$$

$$C_k^1 = \frac{1}{z+1} \sum_{m=-M_k}^{M_k} \left[2(z+1)d_k^2 + (4+3z)e_k d_k + 4(z+1)e_k c_k\right] \qquad (3-A-23)$$

$$C_k^2 = -\frac{1}{z+1} \sum_{m=-M_k}^{M_k} \left[2d_k(b_k+c_k)^2 + zd_k(b_k+c_k)(b_k+2c_k)\right] \qquad (3-A-24)$$

$$C_k^3 = \frac{1}{6(z+1)} \sum_{m=-M_k}^{M_k} \left[(b_k+c_k)^4 + zc_k(b_k+c_k)^3\right] \qquad (3-A-25)$$

$$C_1^0 = \frac{8S(S+1)}{3(2S+1)^6 J^3} \qquad (3-A-26)$$

$$C_2^0 = -C_1^0 \qquad (3-A-27)$$

$$C_1^1 = \frac{1}{z+1}\frac{S}{(2S+1)^5 J^2} \times \qquad (3-A-28)$$
$$\left[-\frac{32+24z}{15}S^4 - \frac{16+12z}{3}S^3 - \frac{8+6z}{3}S^2 + \frac{8+7z}{3}S + \frac{32+29z}{15}\right]$$

$$C_2^1 = \frac{1}{z+1}\frac{S(S+1)}{(2S+1)^5 J^2}\left[\frac{32+24z}{15}S^3 + \frac{16+12z}{5}S^2 - \frac{8+6z}{15}S + \frac{8+11z}{15}\right] \qquad (3-A-29)$$

$$C_1^2 = -\frac{1}{z+1}\frac{S(2S-1)(S+1)}{(2S+1)^4 J}\left[\frac{8+4z}{15}S^3 + \frac{28+16z}{15}S^2 + \frac{32+21z}{15}S + \frac{4+3z}{5}\right] \qquad (3-A-28)$$

$$C_2^2 = \frac{1}{z+1}\frac{S^2(S+1)(2S+3)}{15(2S+1)^4 J}\left[4(z+1)S^2 - 4(z+1)S + z\right] \qquad (3-A-31)$$

$$C_1^3 = \frac{2}{45(z+1)}\frac{S}{(2S+1)^3}(S+1)^3(2S-1)(2S+2+z)(3S^2-\frac{7}{4}) \qquad (3-A-32)$$

$$C_2^3 = \frac{2}{45(z+1)}\frac{S^3}{(2S+1)^3}(2S+3)(S+1)(2S-z)(3S^2+6S+\frac{5}{4}) \qquad (3-A-33)$$

$$D_k^0 = \sum_{m=-M_k}^{M_k} b_k(c_k+b_k) \qquad (3-A-34)$$

$$D_1^0 = \frac{1}{3}S(S+1)(2S-1) \qquad (3-A-35)$$

$$D_2^0 = \frac{1}{3}S(S+1)(2S+3) \qquad (3-A-36)$$

References

1-1) M. E. Fisher, *Physics* **3** (1967) 255, "The Theory of Condensation and the Critical Point."

1-2) M. E. Fisher, *J. Math. Phys.* **2** (1961) 620, "Critical Probabilities for Cluster Size and Percolation Problems."

1-3) R. Kikuchi, *J. Chem. Phys.* **53** (1970) 2713, "Concept of the Long-Range Order in Percolation Problems."

1-4) H. Müller-Krumbhaar, *Phys. Lett.* **48A** (1974) 459, "The Droplet Model in Three Dimensions: Monte Carlo Calculation Results."

1-5) C. Domb, T. Schneider and E. Stoll, *J. Phys.***A8** (1975) L90, "Cluster Shapes in Lattice Gases and Percolation."

1-6) M. F.Sykes and D. S.Gaunt, *J. Phys.* **A9** (1976) 2131, "A Note on the Mean Size of Clusters in the Ising Model."

1-7) K. Binder, *Ann. Phys.* **98** (1976) 390, "Clusters in the Ising Model, Metastable States and Essential Singularity."

1-8) H. E. Stanley, R. J. Birgeneau, P. J. Reynolds and J. F. Nicoll, *J. Phys.* **C9** (1976) L553, "Thermally Driven Phase Transitions Near the Percolation Threshold in Two Dimensions."

1-9) H. E. Stanley, *J. Phys.* **A10** (1977) L211, "Cluster Shapes at the Percolation Threshold "

1-10) N. Jan, A. Coniglio and D. Stauffer, *J. Phys.* **A15** (1982) L699, "Study of Droplets for Correlated Site-Bond Percolation in Two Dimensions."

1-11) D. W. Heermann, A. Coniglio, W. Klein and D. Stauffer, *J. Stat. Phys.* **36** (1984) 447, "Nucleation and Metastability in Three-Dimensional Ising Models."

1-12) C. K. Hu, *Phys. Rev.* **B29** (1984) 5103, "Percolation, Cluster, and Phase Transitions in Spin Models."

1-13) C. K. Hu, *Phys. Rev.* **B32** (1985) 7325, "Geometric Factor and Thermal Properties of a Sublattice Dilute Potts Model."

1-14) For percolation problems see the following reviews:
D. Stauffer, *Phys. Rep.* **54** (1979) 1, "Scaling Theory of Percolation Clusters,"
J. W. Essam, *Rep. Prog. Phys.* **43** (1980) 833, "Percolation Theory."

1-15) K. G. Wilson and M. E. Fisher, *Phys. Rev. Lett.* **28** (1972) 240, "Critical Exponents in 3.99 Dimensions."

1-16) K. G. Wilson and J. Kogut, *Phys. Rep.* **12** (1974) 75, "The Renormalization Group and the ε–Expansion."

1-17) K. G. Wilson, *Rev. Mod. Phys.* **47** (1975) 773, "The Renormalization Group: Critical Phenomena and the Kondo Problem."

1-18) Th. Niemeijer and J. M. J. van Leeuwen, *Phys. Rev. Lett.* **31** (1973) 1411, "Wilson Theory for Spin Systems on a Triangular Lattice."

1-19) B. B. Mandelbrot, *The Fractal Geometry of Nature,* (Freeman and Company, New York, 1977).

42 *References*

1-20) Y. Gefen, B. B. Mandelbrot and A. Aharony, *Phys. Rev. Lett.* **45** (1980) 855, "Critical Phenomena on Fractal Lattices."

1-21) Y. Gefen, A. Aharony, B. B. Mandelbrot and S. Kirkpatrick, *Phys. Rev. Lett.* **47** (1981) 1771, "Solvable Fractal Family, and its Possible Relation to the Backbone at Percolation."

1-22) M. Suzuki, *Prog. Theor. Phys.* **69** (1983) 65, "Phase Transition and Fractals."

1-23) M. E. Fisher and M. N. Barber, *Phys. Rev. Lett.* **28** (1972) 1516, "Scaling Theory for Finite-Size Effects in the Critical Region."

1-24) M. N. Barber,in *Phase Transition and Critical Phenomena, vol.8,* (Academic Press, London, 1983) ed. C. Domb and J. L. Lebowitz.

1-25) M. Suzuki, *Prog. Theor. Phys.* **58** (1977) 1142, "Static and Dynamic Finite-Size Scaling Theory Based on the Renormalization Group Approach."

1-26) K. Binder, *Z. Phys.* **B61** (1985) 13, "Critical Properties and Finite-Size Effects of the Five- Dimensional Ising Model."

1-27) See 1-24) and references therein.

1-28) M. Suzuki, *Prog. Theor. Phys.* **71** (1984) 1397, "Finite-Size Scaling for Transient Similarity and Fractals."

1-29) *Monte Carlo Methods in Statistical Physics,* (Springer-Verlag, 1979) ed. K. Binder.

1-30) K. Binder, *Z. Phys.* **B43** (1981) 119, "Finite Size Scaling Analysis of Ising Model Block Distribution Function."

1-31) R. K. Ghosh and R. E. Shrock, *J. Stat. Phys.* **38** (1985) 473, "Exact Expressions for Row Correlation Functions in the Isotropic d=2 Ising Model."

1-32) B. M. McCoy and T. T. Wu, *The Two-Dimensional Ising Model,* (Harvard, Cambridge, 1973)

1-33) M. Kikuchi and Y. Okabe, *Phys. Rev.* **B35** (1987) 5382, "Renormalization, Self-Similarity and Relaxation of Order– Parameter Structure in Critical Phenomena."

1-34) G. S. Pawley, R. H. Swendsen, D. J. Wallace and K. G. Wilson, *Phys.Rev.* **B29** (1984) 4030, "Monte Carlo Renormalization-Group Calculations of Critical Behavior in the Simple-Cubic Ising Model."

1-35) M. N. Barber, R. B. Pearson, D. Toussaint and J. L. Richardson, *Phys. Rev.* **B32** (1985) 1720, "Finite-Size Scaling in the Three-Dimensional Ising Model."

1-36) J. Adler, *J. Phys.* **A16** (1983) 3565, "Critical Temperatures of the d=3, s=1/2 Ising Model, the Effect of Confluent Corrections to Scaling."

1-37) G. A. Baker, *Phys. Rev.* **B15** (1977) 1552, "Analysis of Hyperscaling in the Ising Model by the High- Temperature Series Methods."

1-38) J. C. LeGuillou and J. Zinn–Justin, *Phys. Rev.* **B21** (1980) 3976, "Critical Exponents from Field Theory."

1-39) M. E. Fisher and D. S. Gaunt, *Phys. Rev.* **A133** (1967) 244, "Ising Model and Self-Avoiding Walks on Hypercubical Lattices and "High Density Expansions."

1-40) T. C. Halsey, M. H. Jensen, L. P. Kadanoff, J. Procaccia and B. I. Shraiman, *Phys. Rev.* **A33** (1986) 1141, "Fractal Measures and their Singularities: the Characterization of Strange Sets."

1-41) J. L. Cambier and M. Nauenberg, N.C.L.C. preprint 1985, "Distribution of Fractal Clusters and Scaling in the Ising Model."

1-42) S. Wansleben, J. G. Zabolitzsky and C. Kalle, *J. Stat. Phys.* **37** (1984) 271, "Monte Carlo Simulation of Ising Models by Multispin Coding on a Vector Computer."

1-43) G. O. Williams and M. H. Kalos, *J. Stat. Phys.* **37** (1984) 283, "A New Multispin Coding Algorithm for Monte Carlo Simulation of the Ising Model."

1-44) G. Bhanot, D. Duke and R. Salvador, *Phys. Rev.* **B33** (1986) 7841, "Finite-Size Scaling and the Three-Dimensional Ising Model."

1-45) G. Bhanot, D. Duke and R. Salvador, *J. Stat. Phys.* **44** (1986) 985, "A Fast Algorithm for the Cyber 205 to Simulate the 3D Ising Model."

1-46) D. E. Knuth, *Seminumerical Algorithms — Random Number, The Art of Computer Programming, vol.2,* (Addison-Wesley)

1-47) R. C. Tausworthe, *Math. Comp.* **19** (1965) 201, "Random Numbers Generated by Linear Recurrence Modulo Two."

1-48) N. Zierler and J. Brillhart, *Inform. Contr.* **13** (1968) 541, "On Primitive Trinomials (Mod 2)."

1-49) N. Zierler and J. Brillhart, *Inform. Contr.* **14** (1968) 566, "On Primitive Trinomials (Mod 2), II."

1-50) J. P. R. Tootill, W. P. Robinson and A. G. Adams, *J. Ass. Comp. Mach.* **18** (1971) 281, "The Runs Up-and-Down Performance of Tausworthe Pseudo-Random Number Generators."

2-1) M. Suzuki and R. Kubo, *J. Phys. Soc. Jpn.* **24** (1968) 51, "Dynamics of the Ising Model Near the Critical Point. 1."

2-2) H. Yahata and M. Suzuki, *J. Phys. Soc. Jpn.* **27** (1969) 1421, "Critical Slowing Down in the Kinetic Ising Model."

2-3) Z. Rácz and M. Collins, *Phys. Rev.* **B13** (1976) 3074, "Linear and Nonlinear Critical Slowing Down in the Kinetic Ising Model: High-Temperature Series."

2-4) H. Takano, *Prog. Theor. Phys.* **68** (1982) 493, "Finite-Size Scaling Approach to the Kinetic Ising Model."

2-5) C. Kalle, *J. Phys.* **A17** (1984) L801, "Vectorised Dynamic Monte Carlo Renormalization Group for the Ising Model."

2-6) S. Miyashita and H. Takano, *Prog. Theor. Phys.* **73** (1985) 1122, "Dynamical Nature of the Phase Transition of the Two- Dimensional Kinetic Ising Model."

2-7) S. Tang and D. P. Landau, *Phys. Rev.* **B36** (1987) 567, "Monte Carlo Study of Dynamic Universality in Two-Dimensional Potts Models,"and references therein.

2-8) H. J. Herrmann, *Physica* **140A** (1986) 421, "Special Purpose Computers in Statistical Physics."

44 *References*

2-9) H. J. Hilhorst, A. F. Bakker, C. Bruim, A. Compagner and A. Hoogland, *J. Stat. Phys.* **34** (1984) 987, "Special Purpose Computers in Physics."

2-10) E. Domany, *Phys. Rev. Lett.* **52** (1984), 87, "Exact Results for Two- and Three-Dimensional Ising and Potts Models."

2-11) *Quantum Monte Carlo Methods,* (Springer, 1987) ed. M. Suzuki.

2-12) *Monte Carlo Methods in Statistical Physics,* (Springer, 1979) ed. K. Binder.

2-13) *Applications of the Monte Carlo Methods in Statistical Physics,* (Springer, 1984) ed. K. Binder.

2-14) D. W. Heermann, *Computer Simulation Methods in Theoretical Physics* (Springer, 1986).

2-15) J. H. Condon and A. T. Ogielski, *Rev. Sci. Instrum.* **56** (1985) 1691, "Fast Special Purpose Computer for Monte Carlo Simulations in Statistical Physics."

2-16) A. T. Ogielski and I. Morgenstern, *Phys. Rev. Lett.* **54** (1985) 928 "Critical Behavior of Three-Dimensional Ising Spin-Glass Model."

2-17) A. T. Ogielski, *Phys. Rev.* **B32** (1985) 7384 "Dynamics of Three-Dimensional Ising Spin Glasses in Thermal Equilibrium."

2-18) A. T. Ogielski, in *Lecture Note in Physics 275* (Springer, 1987).

2-19) A. Hoogland, J. Spaa, B. Selman and A. Compagner, *J. Comp. Phys.* **51** 250 (1983) 250, "A Special-Purpose Processor for the Monte Carlo Simulation of Ising Spin Systems."

2-20) R. Pearson, J. L. Richardson and D. Toussaint, *J. Comp. Phys.* **51** (1983) 241, "A Fast Processor for Monte Carlo Simulation."

2-21) A. Hoogland, A. Compagner and H. W. J. Blöte, *Physica* **132A** (1985) 593, "Smooth Finite-Size Behavior of the Three-Dimensional Ising Model."

2-22) H. W. J. Blöte, A. Compagner, P. A. M. Cornelissen and A. Hoogland, *Physica* **139A** (1985) 395, "Critical Behavior of Two Ising Models with Multispin Interactions."

2-23) H. W. J. Blöte, A. Compagner and A. Hoogland, *Physica* **141A** (1987)375, "The Simple Quadratic Ising Model with Crossing Bonds."

2-24) A. Compagner and A. Hoogland, *J. Comp. Phys.* **71** (1987) 391, "Maximum-Length Sequences, Cellular Automata, and Random Numbers."

2-25) R. Pearson, University of California preprint NSF-ITP-83-62 (1983). "First Results from the Ising Monte Carlo Processor."

2-26) M. N. Barber, R. B. Pearson, D. Toussaint and J. L. Richardson, *Phys. Rev.* **B32** (1985) 1720, "Finite-Size Scaling in the Three-Dimensional Ising Model."

2-27) R. B. Pearson, J. L. Richardson and D. Toussaint, *Phys. Rev.* **B31** (1985) 4472, "Dynamic Correlations in the Three-Dimensional Ising Model."

2-28) J. Beetem, M. Denneau and D. Weingerten, *J. Stat. Phys.* **43** (1986) 1171, "GF11."

2-29) R. C. Tausworthe, *Math. Comp.* **19** (1965) 201, "Random Numbers Generated by Linear Recurrence Modulo Two."

2-30) N. Zierler and J. Brillhart, *Inform. Contr.* **13** (1968) 541, "On Primitive Trinomials (Mod 2)."

2-31) N. Zierler and J. Brillhart, *Inform. Contr.* **14** (1968) 566, "On Primitive Trinomials (Mod 2), II."

2-32) J. P. R. Tootill, W. P. Robinson and A. G. Adams, *J. Ass. Comp. Mach.* **18** (1971) 281, "The Runs Up-and-Down Performance of Tausworthe Pseudo-Random Number Generators."

3-1) M. Suzuki, *J. Phys. Soc. Jpn.* **55** (1986) 4205, "Statistical Mechanical Theory of Cooperative Phenomena 1."

3-2) M. Suzuki, *Phys. Lett.* **116A** (1986) 375, "Coherent Anomalies and an Asymptotic Method in Cooperative Phenomena."

3-3) M. Suzuki, in *Quantum Field Theory,* (Proc. Int. Sympo. Positano, Salerno, Italy, June 5-7, 1985) ed. F.Mancini (North Holland, Amsterdam, 1986).

3-4) M. Suzuki and M. Katori, *J. Phys. Soc. Jpn.* **55** (1986) 1, "New Method to Study Critical Phenomena Mean-Field Finite- Size Scaling Theory."

3-5) M. Suzuki, M. Katori and X. Hu, *J. Phys. Soc. Jpn.* **56** (1987) 3092, "Coherent-Anomaly Method in Critical Phenomena I."

3-6) M. Katori and M. Suzuki, *J. Phys. Soc. Jpn.* **56** (1987) 3113, "Coherent-Anomaly Method in Critical Phenomena II."

3-7) X. Hu, M. Katori and M. Suzuki, *J. Phys. Soc. Jpn.* **56** (1987) 3865, "Coherent-Anomaly Method in Critical Phenomena III."

3-8) X. Hu and M. Suzuki, *J. Phys. Soc. Jpn.* **57** (1988) No.3, "Coherent-Anomaly Method in Critical Phenomena IV."

3-9) M. Suzuki, preprint (submitted to *Phys. Lett. A.*) "CAM estimates of Critical Exponents of Spin Glass and Percolation."

3-10) H. Takayasu and M. Takayasu, preprint, "Application of the Coherent Anomaly Method to Percolation."

3-11) M. Suzuki, *J. Phys. Soc. Jpn.* **56** (1987) 4221, "Power-Series CAM Theory."

3-12) M. Suzuki, *J. Phys. Soc. Jpn.* **57** (1988) 1, "Continued-Fraction CAM Theory of Critical Phenomena."

3-13) P. R. Weiss, *Phys. Rev.* **74** (1948) 1493, "The Application of the Bethe-Peierls Method to Ferromagnetism."

I find three misprints in this paper. In eq. (55), A and B should be interchanged. The factor $1/(2n+1)$ in the LHS of eq.(58) should read $(2n+1)$. The RHS of the last equation in Eq.(38) should be $T(T+1)(2T+1)(3T^2+3T-1)/15$.

3-14) P. W. Kasteleijn and J. van Kranendonk, *Physica* **22** (1956) 317, "Constant Coupling Approximation for Heisenberg Ferromagnetism."

3-15) G. S. Rushbrooke, G. A. Baker, Jr. and P. J. Wood in *Phase Transition and Critical Phenomena, vol. 3,* (Academic Press London, 1974) ed. C.Domb and M.S.Green.

3-16) M. Suzuki, *Prog. Theor. Phys. Supp.* **87** (1986) 1, "Skeletonization, Fluctuation Mean-Field Approximations and Coherent Anomalies in Critical Phenomena."